

# Analyzing the Motion of a Washer on a Rod

Hiroshi Takano<sup>1</sup>

<sup>1</sup>*Educational Studies on Global-ICT-Teaching and Learning, Joetsu University of Education  
1 Yamayashiki-cho, Joetsu, Niigata, 943-8512, Japan\**

(Dated: Mar. 11, 2023)

This paper investigates the dynamics of a toy known as the chatter ring. Specifically, it examines the mechanism by which the small ring rotates around the large ring, the mechanism by which the force from the large ring provides torque to the small ring, and whether the motion of the small ring is the same as that of a hula hoop. The dynamics of a chatter ring has been investigated in previous work [13, 14, 15]; however, a detailed analysis has not yet been performed. Thus, to understand the mechanisms described above, the equations of motion and constraint conditions are obtained, and an analysis of the motion is performed. To simplify the problem, a model consisting of a straight rod and a washer ring is analyzed under the no-slip condition. The motion of a washer has two modes: the one point of contact (1PC) mode and two points of contact (2PC) mode. The motion of the small ring of the chatter ring is similar to that of a washer in the 2PC mode, whereas the motion of a hula hoop is similar to that of a washer in the 1PC mode. The analysis indicates that the motion of a washer with two points of contact is equivalent to free fall motion. However, in practice, the velocity reaches a constant value through energy dissipation. The washer rotates around an axis that passes through the two points of contact. The components of the forces exerted by the rod at the points of contact that are normal to the plane of the washer provide rotational torque acting at the center of mass. The components of the forces parallel to the horizontal plane are centripetal forces, which induce the circular motion of the center of mass.

## I. INTRODUCTION

Some toys, such as tip tops and rattlebacks [1, 2, 3, 4], exhibit curious and interesting behavior. A chatter ring, also known as a jitter ring or gyro ring, is a toy with a large loop made from a metal rod on which there are small rings, as illustrated in Fig. 1(a). Like the aforementioned toys, the small rings of a chatter ring also exhibit interesting behavior.

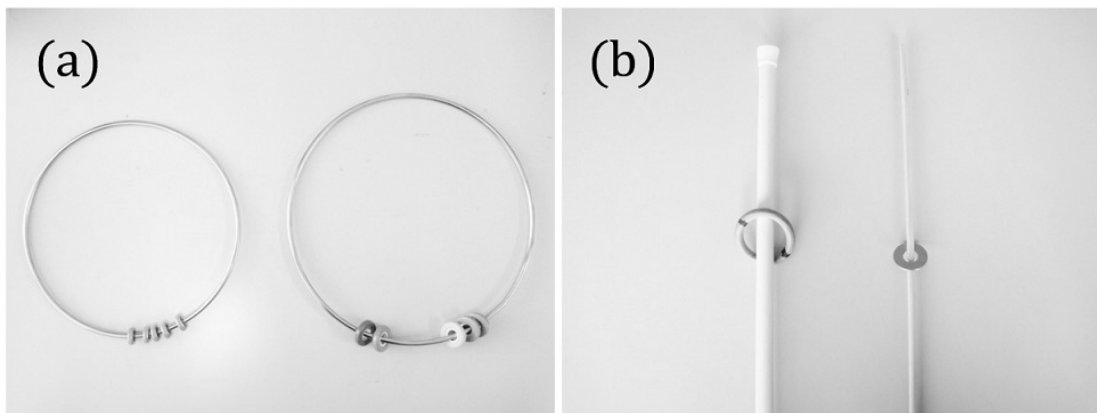


FIG. 1. (a) Jitter ring and gyro ring. (b) Rod with a torus-shaped ring (left) and rod with a washer (right).

The chatter ring is played with as follows. First, rotation of the small rings is initiated by hand, and then the large ring is rotated by hand to apply a constant rotation to the small rings. The purpose of playing with a chatter ring is not only to keep the small rings rotating, but also to learn various skills with different levels of difficulty. After learning individual skills, combining them can result in impressive performances. Videos of such performances have been uploaded to the Japan Chatter Ring Association [5] website and to YouTube.

---

\* Email: takano@juen.ac.jp

A phenomenon similar to that of chatter ring motion can be observed in the artwork of K. Sato [6]. For example, the work *Over the Waves* (1974) contains three wires, and a wire shaped like a wave is attached to a plate. A small ring on the wire is rotated by an electromagnetic force provided by the coil of a motor hidden under the plate. The small ring moves to the edge of the plate and then returns in the opposite direction. The principle of the motion of the small ring is considered to be the same as that of the chatter ring.

The motion of the small ring of a chatter ring is not well understood. Specifically, it is unclear how the small ring rotates around the large ring, how the large ring provides torque to the small ring, and whether the motion of the small ring is the same as that of a hula hoop [7]. The motion is predicted easily to be caused by the frictional force between the large ring and small ring. But it is necessary to produce and analyze the equations of motion in order to understand the magnitude and direction of that force in detail.

Tip tops and rattlebacks spin on a flat plane, whereas in a chatter ring, the small ring spins on the curved surface of the large ring. Thus, the analysis of a chatter ring is more difficult than that of a rattleback. The rolling behavior of a rigid body moving on a sphere has been studied [8], and the equations of motion of a rigid body have been presented for arbitrary body and surface shapes. An example of the motion of a rigid body moving on a curved surface is the motion of a ball rolling inside a cylinder. This problem has been discussed in the literature [9, 10, 11, 12]; however, the behavior of a rigid body, such as the small ring of a chatter ring, has not yet been studied.

Considering the motion of the large ring makes the analysis of the motion of the small ring difficult. As the motion of the large ring only serves to the height of the small ring fixed, we can replace the large ring with a long rod. We can then analyze a model that consists of a fixed long rod and small ring, as illustrated in Fig. 1(b). We assume that the motion of the ring on the rod is essentially the same as that of the small ring of a chatter ring. In fact, photographing these motions with a high-speed camera and comparing them indicates that they are almost the same. Using the model consisting of the long rod allows us to perform experiments with rods of various thicknesses and rings with various inner diameters, thereby enabling detailed analysis of the dynamics [13].

The motion of the small ring has two modes [14]. One is rotation while remaining in a fixed position with one point of contact (1PC mode). This motion is similar to that of a hula hoop and a ball rolling inside a cylinder [11, 12]. The second mode is movement in one direction while rotating with two points of contact (2PC mode). This movement is similar to that of the small ring of a chatter ring. The trace of the two points of contact is a double helix on the rod surface [15]. Videos of these modes of motion are available on the website of Hunt [14].

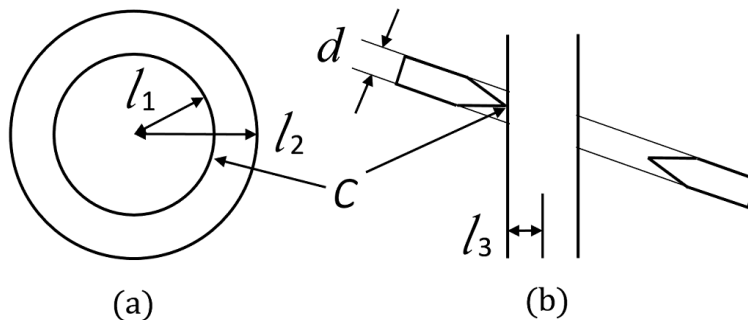


FIG. 2. Rod and washer ring whose inner diameter has a sharp tip. (a)  $l_1$  is the radius of the inner circle  $C$  of the ring, while  $l_2$  is the radius of the outer circle of the ring. (b)  $l_3$  is the radius of the rod and the  $d$  is the thickness of the washer.

For a torus-shaped ring or thick washer, it is possible but difficult to determine the position of the point of contact, thus complicating the analysis of the equations of motion. Therefore, we consider a special washer ring whose inner diameter has a sharp tip. The shapes of the washer and rod are illustrated in Fig. 2. We fix the point of contact with one parameter because the point is on a one-dimensional circle. Using only one parameter makes the analysis of the equations of motion simpler than in the case of a torus-shaped ring. The radius of the inner circle  $C$  of the ring is  $l_1$ , while the radius of the outer circle of the ring is  $l_2$ , as indicated in Fig. 2(a). The radius of the rod is  $l_3$ , as illustrated in Fig. 2(b).

In this paper, we obtain the equations of motion of the washer and rod system when the washer ring moves with one point of contact and two points of contact. We then analyze the motion to clarify the dynamics of the chatter ring.

## II. WASHER AND ROD SYSTEM

### A. Angles between frames that define the configuration of the washer

The washer and rod system is illustrated in Fig. 3. The unit vectors of the principal axes of inertia are  $\bar{e}_i (i = 1, 2, 3)$ , and the frame  $\bar{E}_i (i = 1, 2, 3)$  is fixed to the rod. The point of contact is denoted by  $P$ , the origin of the frame  $\bar{E}_i$  is denoted by  $O$ , and the origin of the frame  $\bar{e}_i$  is the center of mass denoted by  $G$ . The position vectors are  $\mathbf{r}_t = \overrightarrow{OP}$ ,  $\mathbf{r}_g = \overrightarrow{OG}$ , and  $\mathbf{r} = \overrightarrow{GP}$ . These vectors are related by the following equation:

$$\mathbf{r}_g = \mathbf{r}_t - \mathbf{r}. \quad (1)$$

To obtain the angular velocity  $\boldsymbol{\omega}$ , we require a matrix  $R$  that relates  $\bar{e}_i$  to  $\bar{E}_i$ , such as

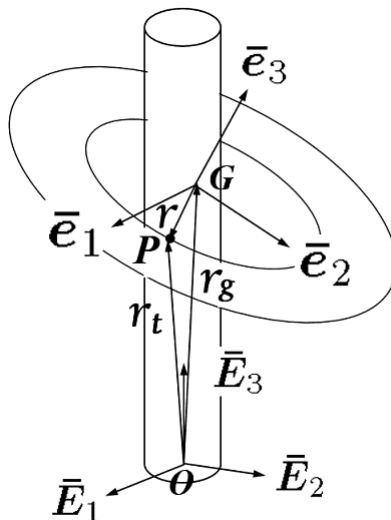


FIG. 3. Washer and rod system.  $P$  denotes the point of contact. The position vectors are  $\mathbf{r} = \overrightarrow{GP}$ ,  $\mathbf{r}_t = \overrightarrow{OP}$ , and  $\mathbf{r}_g = \overrightarrow{OG}$ . The unit vectors of the principal axes of inertia are  $\bar{e}_i (i=1,2,3)$ , and  $\bar{E}_i (i=1,2,3)$  represents the frame fixed to the rod.

$$\bar{e}_i = R_{ij} \bar{E}_j. \quad (2)$$

First, as illustrated in Fig. 4(a), we set  $\bar{E}_i = \bar{e}_i$ , and the point of contact  $P$  is on the  $\bar{e}_1$  axis. Then, the washer is rotated by an angle  $\phi$  around the axis  $\bar{e}_3$  without slipping. The point of contact moves to position  $P$ , where the angle between the position vector  $\overrightarrow{GP}$  and unit vector  $\bar{e}_1$  is  $\phi$ . The unit vector on the line  $GP$  is denoted by  $\mathbf{e}_1^{(a)}$ . The axis  $\mathbf{e}_2^{(a)}$  is obtained by rotating the axis  $\bar{e}_2$  by  $\phi$ . Point  $P'$  is a point obtained by projecting point  $P$  onto the  $\bar{E}_1, \bar{E}_2$  plane, and we set the unit vector  $\mathbf{E}_1$  on the line  $OP'$ .  $\eta$  denotes the angle between  $\bar{E}_1$  and  $\mathbf{E}_1$ . Next, the washer is rotated by an angle  $\psi$  around axis  $\mathbf{e}_1^{(a)}$ . The axes after rotation by an angle  $\psi$  are denoted by  $\mathbf{e}_i^{(b)}$  as illustrated in Fig. 4(b). The dotted lines represent the original axes  $\mathbf{e}_i^{(a)}$  before the rotation. Lastly, the washer is rotated by an angle  $\theta$  around axis  $\mathbf{e}_2^{(b)}$  without moving the point of contact  $P$ . The axes after rotation  $\theta$  are denoted by  $\mathbf{e}_i$  as displayed in Fig. 4(c). Fig. 4(d) presents the motion of the axes rotated by an angle  $\theta$  after rotation by an angle  $\psi$ .

The axes are related as follows:

$$\mathbf{e}_i = R_{3\phi ij} \bar{e}_j, \quad (3)$$

$$\mathbf{E}_i = R_{3\eta ij} \bar{E}_j, \quad (4)$$

$$\mathbf{E}_i = R_{1\psi ij} R_{2\theta jk} \mathbf{e}_k, \quad (5)$$

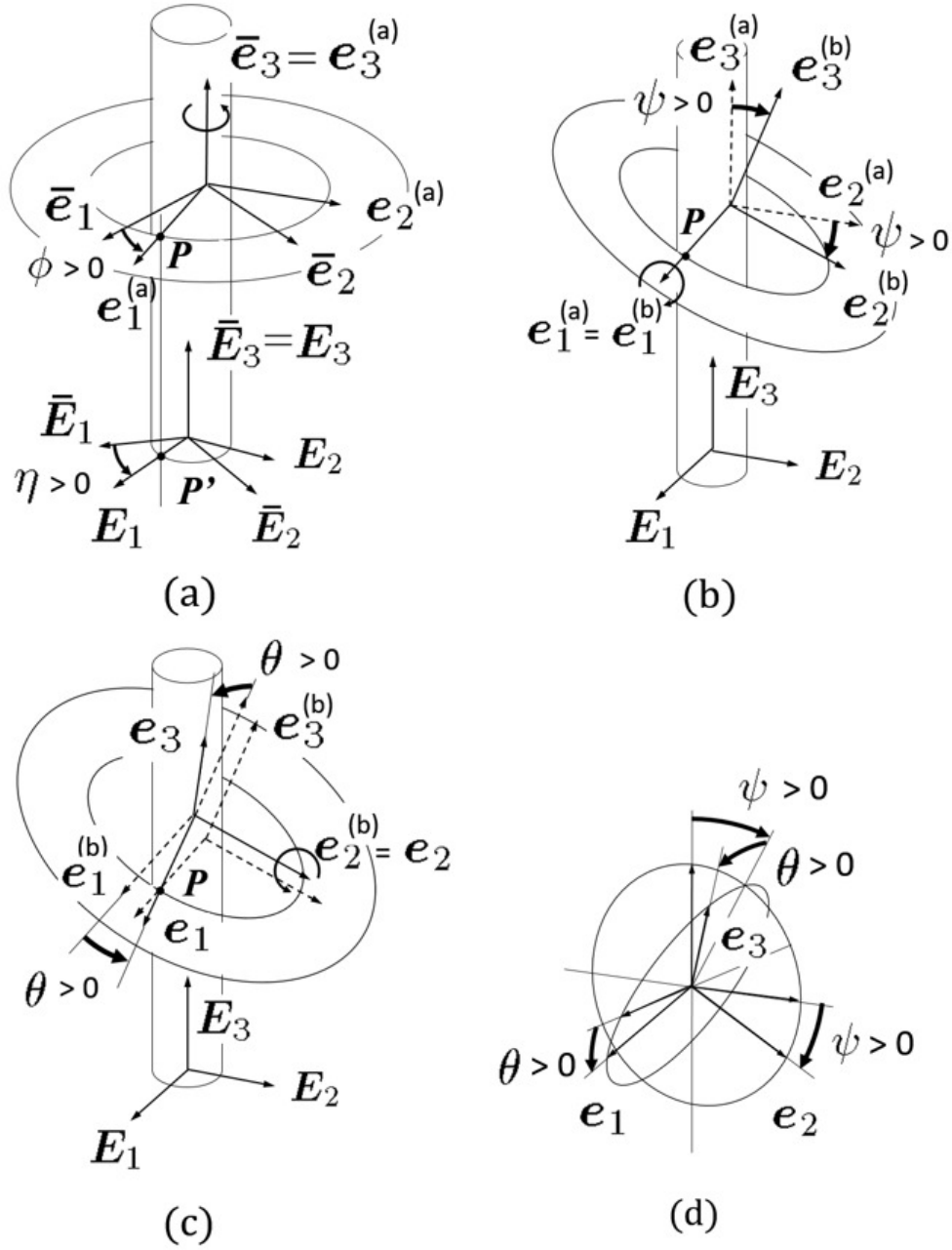


FIG. 4. (a)  $\phi$  is the angle between  $\bar{e}_1$  and the rotated axis  $e_1^{(a)}$ , while  $\eta$  is the angle between  $\bar{E}_1$  and the rotated axis  $E_1$ . (b)  $\psi$  is the angle between the axes  $e_{2,3}^{(a)}$  and the rotated axes  $e_{2,3}^{(b)}$ . (c)  $\theta$  is the angle between the axes  $e_{1,3}^{(b)}$  and the rotated axes  $e_{1,3}$ . (d) Motion of the axes rotated by an angle  $\theta$  after rotation by an angle  $\psi$ .

where

$$\begin{aligned}
 R_{3\phi} &\equiv \begin{pmatrix} \cos \phi & \sin \phi & 0 \\ -\sin \phi & \cos \phi & 0 \\ 0 & 0 & 1 \end{pmatrix}, & R_{3\eta} &\equiv \begin{pmatrix} \cos \eta & \sin \eta & 0 \\ -\sin \eta & \cos \eta & 0 \\ 0 & 0 & 1 \end{pmatrix}, \\
 R_{1\psi} &\equiv \begin{pmatrix} 1 & 0 & 0 \\ 0 & \cos \psi & \sin \psi \\ 0 & -\sin \psi & \cos \psi \end{pmatrix}, & R_{2\theta} &\equiv \begin{pmatrix} \cos \theta & 0 & \sin \theta \\ 0 & 1 & 0 \\ -\sin \theta & 0 & \cos \theta \end{pmatrix}.
 \end{aligned} \tag{6}$$

Thus, we obtain the relation between  $\bar{e}_i$  and  $\bar{\mathbf{E}}_i$  as

$$\bar{\mathbf{e}} = R\bar{\mathbf{E}}, \quad R \equiv R_{3\phi}^{-1}R_{2\theta}^{-1}R_{1\psi}^{-1}R_{3\eta}, \quad (7)$$

where we omit the subscript of the matrix. The connection between two reference frames is parametrized by three Euler angles, although it appears to be described by four independent parameters in Eq. (7). There are still three independent parameters since eta, phi, and psi are related by the no-slip condition Eq. (31), which we will see later in Section III A. It is suitable to describe the configuration of a rigid body with four parameters and then impose constraint conditions, in order to describe it that moves without slipping on the surface of a curved rod.

The order of rotation is important. If the washer is first rotated by an angle  $\theta$  around the  $e_2^{(a)}$  axis as illustrated in Fig. 5(a) after the  $\phi$  rotation, then it must be rotated by an angle  $\psi$  around the  $e_1^{(a)} = \mathbf{E}_1$  axis perpendicular to the surface of rod, but not around the  $e_1^{(b)}$  axis as illustrated in Fig. 5(b). If the washer is rotated around the  $e_1^{(b)}$  axis, the washer gets stuck. The  $e_3^{(a)} = \mathbf{E}_3$  axis, the  $e_3^{(b)}$  axis, the  $e_1^{(a)} = \mathbf{E}_1$  axis and the  $e_1^{(b)}$  axis are in the same plane as illustrated in Fig. 5(c). Thus it can be seen that  $\mathbf{E}_3^{(b)}$ ,  $e_3$ ,  $e_1^{(a)} = \mathbf{E}_1$  and  $e_1$ , which are obtained by rotating these axes around the  $e_1^{(a)} = \mathbf{E}_1$  axis, are also in the same plane as illustrated in Fig. 5(c). Moreover, it can be seen that  $\mathbf{E}_3$ ,  $\mathbf{E}_3^{(b)}$ ,  $\mathbf{E}_2$  and  $e_2$  are in the same plane as illustrated in Fig. 5(c). Thus, we have the relation equations below

$$\mathbf{E}_1 = \cos\theta e_1 + \sin\theta e_3, \quad (8)$$

$$\mathbf{E}_3^{(b)} = -\sin\theta e_1 + \cos\theta e_3, \quad (9)$$

$$\mathbf{E}_2 = \cos\psi e_2 + \sin\psi \mathbf{E}_3^{(b)}, \quad (10)$$

$$\mathbf{E}_3 = -\sin\psi e_2 + \cos\psi \mathbf{E}_3^{(b)}. \quad (11)$$

Substitution of Eq. (9) into Eq. (10) and Eq. (11) yields the following equations:

$$\mathbf{E}_2 = -\sin\psi e_1 + \cos\psi e_2 + \sin\psi \cos\theta e_3, \quad (12)$$

$$\mathbf{E}_3 = -\cos\psi \sin\theta e_1 - \sin\psi e_2 + \cos\psi \cos\theta e_3. \quad (13)$$

We find that the relation equations Eq. (8), Eq. (12) and Eq. (13) between the  $e_i$  axes and the  $\mathbf{E}_i$  axes are the same as Eq. (5).

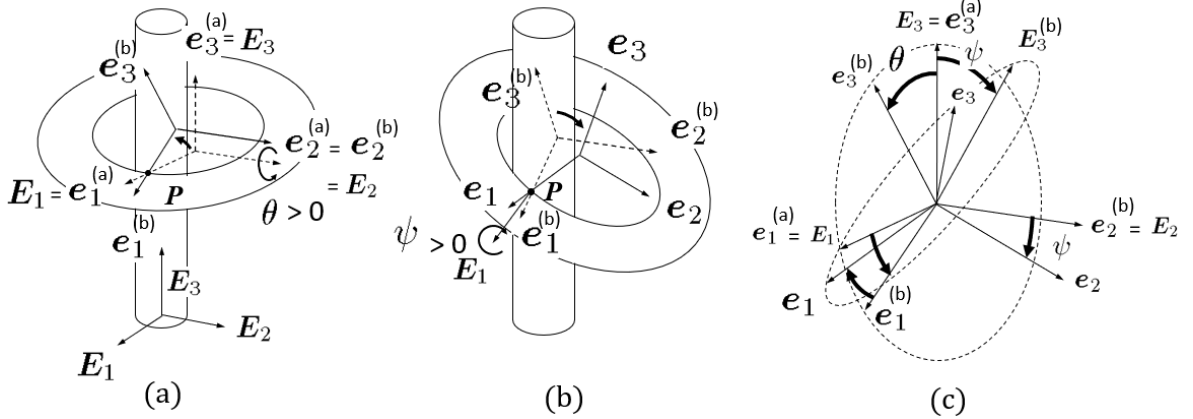


FIG. 5. (a)  $\theta$  is the angle between  $e_{1,3}^{(a)}$  and the rotated axis  $e_{1,3}^{(b)}$ .  $e_2^{(a)} = e_2^{(b)} = \mathbf{E}_2$  is the axis of rotation. (b) Dashed vectors are  $e_i^{(b)}$  frame.  $\psi$  is the rotation angle around the  $\mathbf{E}_1$ . (c) Motion of the axes rotated by an angle  $\psi$  after rotation by an angle  $\theta$ .

We present several examples of washer configurations. Fig. 6 illustrates the washer system at a positive value of  $\theta$  and  $\psi = 0$ . Fig. 6(1) indicates that there is one point of contact, while Fig. 6(1)(a) presents the view from above and the curved line  $C_1$ , which is obtained by projection of the inner circle of washer  $C$  onto the plane defined by unit vectors  $\mathbf{E}_1$  and  $\mathbf{E}_2$ . Fig. 6(1)(b) presents the view from the direction parallel to  $e_1$ , while Fig. 6(1)(c) presents the view from the side. Fig. 6(2) illustrates the washer configuration that has two points of contact,  $P$  and  $\bar{P}$ , at the value of  $\theta_c > 0$ . The value of  $\theta_c$  is determined in Section IV B. Fig. 6(3) presents an unrealistic situation at the value of

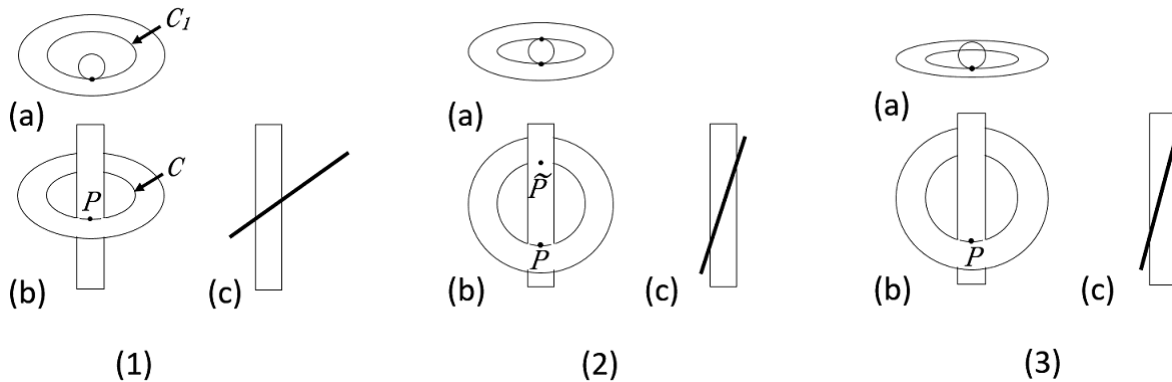


FIG. 6. Washer configurations at  $\psi = 0, \theta \geq 0$ . (1) One point of contact,  $P$ .  $C_1$  is a curved line which is obtained by projection of the inner circle of washer  $C$  onto the plane defined by unit vectors  $\mathbf{E}_1$  and  $\mathbf{E}_2$ . (2) Two points of contact,  $P$  and  $\tilde{P}$ , at the value of  $\theta_c > 0$ . (3) Unrealistic situation at the value of  $\theta > \theta_c$  in which the washer gets stuck in the rod.

$\theta > \theta_c$  in which the washer gets stuck in the rod. In each of the subfigures of Fig. 6, the view from above is displayed in (a), the view from the direction parallel to  $\mathbf{e}_1$  is displayed in (b), and the view from the side is displayed in (c).

Fig. 7 displays washer configurations at a positive value of  $\psi$  and  $\theta = 0$ . Fig. 7(1) indicates that there is only one point of contact, while Fig. 7(2) illustrates the configuration with  $\psi_c$  where the curvature of  $C_1$  at point  $P$  is equal to that of the rod. The value of  $\psi_c$  is determined in Section IV B. When the absolute value of  $\psi$  becomes larger than  $\psi_c$ , the washer gets stuck in the rod, as illustrated in Fig. 7(3).

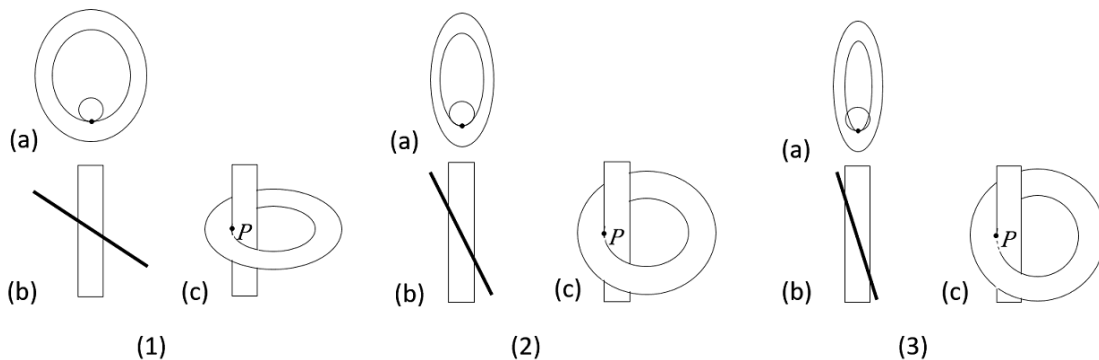


FIG. 7. Washer configurations at  $\theta = 0, \psi \geq 0$ . (1) One point of contact,  $P$ . (2) Configuration with  $\psi_c$  where the curvature of  $C_1$  at point  $P$  is equal to that of the rod. (3) When the absolute value of  $\psi$  becomes larger than  $\psi_c$ , the washer gets stuck in the rod.

We observe the configuration of the washer at a value of  $\psi$  and  $\theta$ . Fig. 8 presents configurations when  $\theta > 0$ . Fig. 8(1) presents the configuration with two points of contact while Fig. 8(2) presents the configuration with one point of contact when  $\psi < 0$ . Fig. 8(3) presents the configuration with one point of contact while Fig. 8(4) presents the configuration with two points of contact when  $\psi > 0$ . In Fig. 8(1), when  $\dot{\phi} > 0$ , it follows from Eq. (32) that the washer moves upward, while in Fig. 8(4), the washer moves downward. Fig. 9 presents configurations when  $\theta < 0$ . Fig. 9(1) presents the configuration with two points of contact while Fig. 9(2) presents the configuration with one point of contact when  $\psi > 0$ . Fig. 9(3) presents the configuration with one point of contact while Fig. 9(4) presents the configuration with two points of contact when  $\psi < 0$ . In Fig. 9(1), when  $\dot{\phi} > 0$ , it follows from Eq. (32) that the washer moves upward, while in Fig. 9(4), the washer moves downward. Figs. 8(1) and 9(1) display the same configuration, and Figs. 8(4) and 9(4) also display the same configuration.

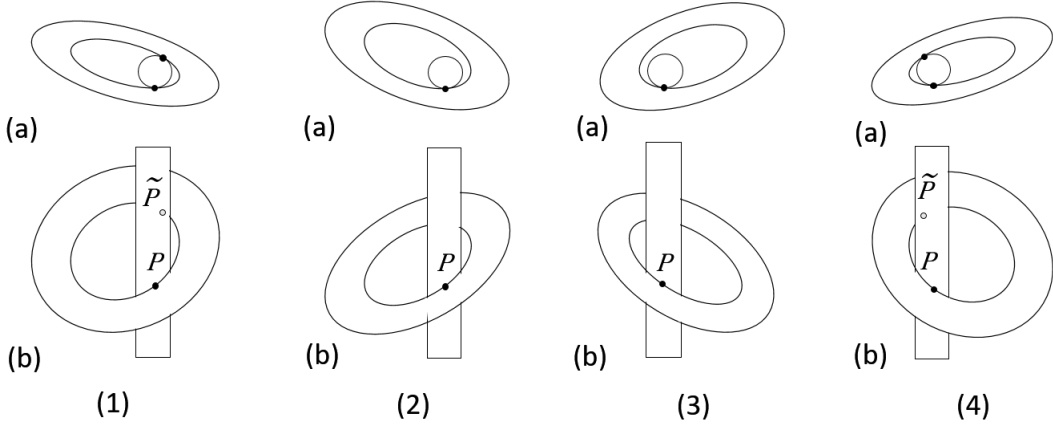


FIG. 8. Washer configurations at  $\theta > 0$ . (1) Configuration with two points of contact,  $P$  and  $\tilde{P}$  when  $\psi < 0$ . (2) Configuration with one point of contact,  $P$  when  $\psi < 0$ . (3) Configuration with one point of contact,  $P$  when  $\psi > 0$ . (4) Configuration with two points of contact,  $P$  and  $\tilde{P}$  when  $\psi > 0$ .

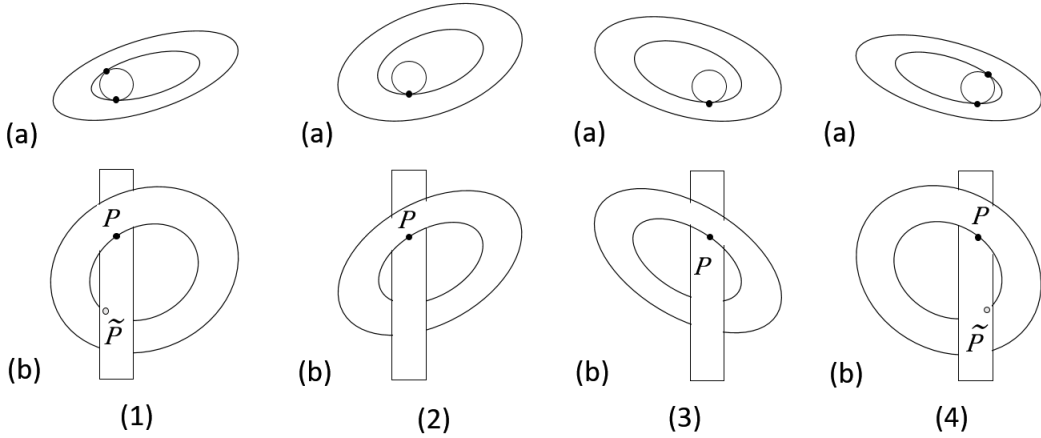


FIG. 9. Washer configurations at  $\theta < 0$ . (1) Configuration with two points of contact,  $P$  and  $\tilde{P}$  when  $\psi < 0$ . (2) Configuration with one point of contact,  $P$  when  $\psi < 0$ . (3) Configuration with one point of contact,  $P$  when  $\psi > 0$ . (4) Configuration with two points of contact,  $P$  and  $\tilde{P}$  when  $\psi > 0$ .

## B. Vector Components

We examine the relation between the components of vector  $\mathbf{A}$  with different coordinates. There is a relation between the coordinate frame  $\mathbf{x}$  and  $\mathbf{y}$ , given by

$$\mathbf{y}_i = K_{ij} \mathbf{x}_j.$$

The component of vector  $\mathbf{A}$  is denoted by  $\alpha_i$  ( $\beta_i$ ) with respect to the frame  $\mathbf{x}$  ( $\mathbf{y}$ ), and in the following discussion, we use the notation

$$\mathbf{A} = (\alpha_1, \alpha_2, \alpha_3)_{\mathbf{x}} = (\beta_1, \beta_2, \beta_3)_{\mathbf{y}}.$$

Vector  $\mathbf{A}$  is expressed as

$$\mathbf{A} = \alpha_j \mathbf{x}_j = \beta_i \mathbf{y}_i = \beta_i K_{ij} \mathbf{x}_j.$$

Then, using  $K^{-1} = K^t$ , we have the relation

$$\alpha_j = \beta_i K_{ij}, \quad \beta_i = K_{ij} \alpha_j. \quad (14)$$

This relation indicates that the transformation rule of the components has the same form as that of the coordinate frame. Thus, we obtain the relation equations between the components in each coordinate,  $\mathbf{A} = (a_i)_e = (\bar{a}_i)_{\bar{e}} = (A_i)_E = (\bar{A}_i)_{\bar{E}}$ , as follows:

$$a_i = R_{3\phi ij} \bar{a}_j, \quad (15)$$

$$A_i = R_{3\eta ij} \bar{A}_j, \quad (16)$$

$$A_i = R_{1\psi ij} R_{2\theta jk} a_k. \quad (17)$$

The time derivative of vector  $\mathbf{A} = (\bar{a}_1, \bar{a}_2, \bar{a}_3)_{\bar{e}} = (a_1, a_2, a_3)_e$  is given by

$$\frac{d}{dt} \mathbf{A} = \left( \frac{d}{dt} \bar{a}_i \right) \bar{e}_i + \boldsymbol{\omega} \times \mathbf{A}. \quad (18)$$

When we obtain the components of the equation of motion, the expression  $\frac{d}{dt} \mathbf{A}$  with respect to components  $a_i$  and  $\omega_i$  of frame  $e$  is useful. The first term on the right hand side of Eq. (18) contains a term proportional to  $\dot{\phi}$  and is given by

$$\begin{aligned} \left( \frac{d}{dt} \bar{a}_i \right) \bar{e}_i &= \frac{d}{dt} \left( R_{3\phi ij}^{-1} a_j \right) R_{3\phi ik}^{-1} e_k = \left( \left( \frac{d}{dt} R_{3\phi ij}^{-1} \right) a_j + R_{3\phi ij}^{-1} \dot{a}_j \right) R_{3\phi ik}^{-1} e_k \\ &= \left( a_j \left( \frac{d}{dt} R_{3\phi ji} \right) + \dot{a}_j R_{3\phi ji} \right) R_{3\phi ik}^{-1} e_k \\ &= ((a_1, a_2, a_3)_e \begin{pmatrix} -\dot{\phi} \sin \phi & \dot{\phi} \cos \phi & 0 \\ -\dot{\phi} \cos \phi & -\dot{\phi} \sin \phi & 0 \\ 0 & 0 & 0 \end{pmatrix} + \dot{a}_j R_{3\phi ji}) R_{3\phi ik}^{-1} e_k \\ &= (\dot{a}_1 - \dot{\phi} a_2, \dot{a}_2 + \dot{\phi} a_1, \dot{a}_3)_e, \end{aligned} \quad (19)$$

where  $\dot{a}_i \equiv \frac{d}{dt} a_i$ , and we use Eq. (15) and the relations  $\bar{a} = R_{3\phi}^{-1} a$  and  $R_{3\phi}^{-1} = R_{3\phi ji}$ . The second term on the right hand side of Eq. (18) is given by

$$\boldsymbol{\omega} \times \mathbf{A} = (\omega_2 a_3 - \omega_3 a_2, \omega_3 a_1 - \omega_1 a_3, \omega_1 a_2 - \omega_2 a_1)_e, \quad (20)$$

where the components of the angular velocity  $\boldsymbol{\omega}$  are represented by  $\boldsymbol{\omega} = (\bar{\omega}_1, \bar{\omega}_2, \bar{\omega}_3)_{\bar{e}} = (\omega_1, \omega_2, \omega_3)_e$ . The components of the angular momentum  $\mathbf{L}$  are represented by  $\mathbf{L} = (\bar{L}_1, \bar{L}_2, \bar{L}_3)_{\bar{e}} = (L_1, L_2, L_3)_e$ . In addition,  $\bar{L}_i$  represents the angular momentum along the principal axis of inertia. These components relate to the angular velocity  $\bar{\omega}_i$  as follows:

$$\bar{L}_1 = \bar{I}_1 \bar{\omega}_1, \quad \bar{L}_2 = \bar{I}_1 \bar{\omega}_2, \quad \bar{L}_3 = \bar{I}_3 \bar{\omega}_3, \quad (21)$$

where  $\bar{I}_i (i=1,2,3)$  represents the principal moments of inertia for each principal axis of inertia, and we use  $\bar{I}_1 = \bar{I}_2$ . The values  $L_i$  are given as

$$\begin{aligned} L_1 &= \cos \phi \bar{L}_1 + \sin \phi \bar{L}_2 = \bar{I}_1 (\cos \phi \bar{\omega}_1 + \sin \phi \bar{\omega}_2) = \bar{I}_1 \omega_1, \\ L_2 &= -\sin \phi \bar{L}_1 + \cos \phi \bar{L}_2 = \bar{I}_1 \omega_2, \quad L_3 = \bar{I}_3 \omega_3, \end{aligned} \quad (22)$$

where we use the relations  $L_i = R_{3\phi ij} \bar{L}_j$  and  $\omega_i = R_{3\phi ij} \bar{\omega}_j$ .

Lastly, we obtain the time derivative of the angular momentum:

$$\begin{aligned} \frac{d}{dt} \mathbf{L} &= (\dot{L}_1 - \dot{\phi} L_2, \dot{L}_2 + \dot{\phi} L_1, \dot{L}_3)_e + (\omega_2 L_3 - \omega_3 L_2, \omega_3 L_1 - \omega_1 L_3, \omega_1 L_2 - \omega_2 L_1)_e \\ &= (\bar{I}_1 (\dot{\omega}_1 - \dot{\phi} \omega_2) - (\bar{I}_1 - \bar{I}_3) \omega_2 \omega_3, \bar{I}_1 (\dot{\omega}_2 + \dot{\phi} \omega_1) - (\bar{I}_3 - \bar{I}_1) \omega_3 \omega_1, \bar{I}_3 \dot{\omega}_3)_e. \end{aligned} \quad (23)$$

### III. MOTION OF THE WASHER WITH ONE POINT OF CONTACT

#### A. No-slip Condition

We consider the rolling motion of a rigid body  $A$  without slipping on the surface of a rigid body  $B$  fixed to a desk or table, as illustrated in Fig. 10(a). The principal central axes of inertia of the body  $A$  are  $\bar{e}_i$ , while  $O_A$  is the center

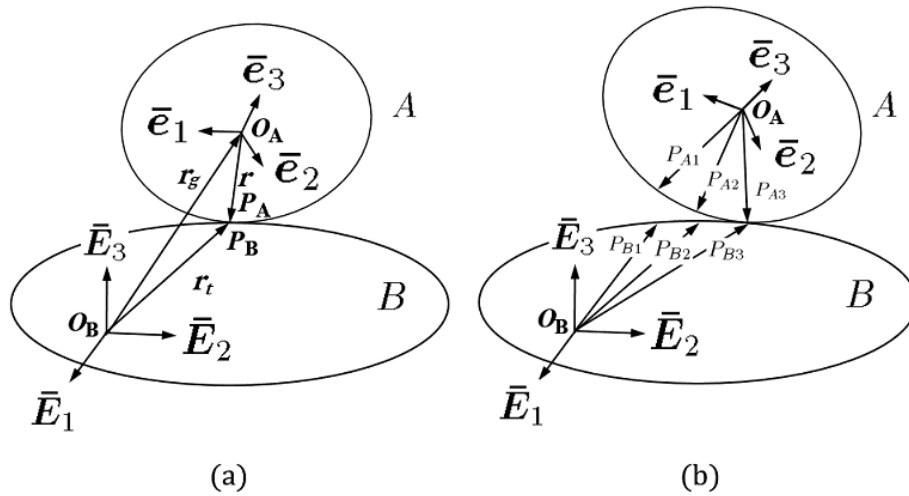


FIG. 10. Rolling motion of rigid body A without slipping on the surface of rigid body B. (a) Bodies A and B. (b) Locus of the points of contact  $P_A$  and  $P_B$  fixed to bodies A and B.

of mass of A. An absolute coordinate frame  $\bar{\mathbf{E}}_i$  is fixed to body B, and the origin is denoted by  $O_B$ . Points  $P_A$  and  $P_B$  refer to the point of contact  $P$  on the surface of bodies A and B, respectively.

The position vectors of the point of contact  $P$  from origin  $O_A$  and origin  $O_B$  are denoted by  $\mathbf{r}$  and  $\mathbf{r}_t$ , respectively. The position vector of the center of mass  $O_A$  from origin  $O_B$  is denoted by  $\mathbf{r}_g$ .

If body A moves on the surface of body B without slipping, the loci of the points of contact  $P_A$  and  $P_B$  are obtained by  $P_{A1}, P_{A2}, P_{A3}$  and  $P_{B1}, P_{B2}, P_{B3}$  in Fig. 10(b), respectively. The position vector  $\mathbf{r}$  has the coordinate  $\mathbf{r} = \bar{r}_i(t)\bar{\mathbf{e}}_i(t)$ . The velocity of  $P_A$ , which is denoted by  $\mathbf{v}_A$ , is obtained by moving with the coordinate  $\bar{\mathbf{e}}_i(t)$  and is thus

$$\mathbf{v}_A = \left( \frac{d}{dt} \bar{r}_i(t) \right) \bar{\mathbf{e}}_i(t). \quad (24)$$

Similarly, the vector  $\mathbf{r}_t = \bar{r}_{ti}(t)\bar{\mathbf{E}}_i$  moves on the surface of B along the locus  $P_{B1}, P_{B2}, P_{B3}$ . In the same way, the velocity of  $P_B$ , denoted by  $\mathbf{v}_B$ , is given by

$$\mathbf{v}_B = \left( \frac{d}{dt} \bar{r}_{ti}(t) \right) \bar{\mathbf{E}}_i. \quad (25)$$

Without slipping, the equation for the constraint condition

$$\mathbf{v}_A = \mathbf{v}_B \quad (26)$$

is satisfied, and the direction of  $\mathbf{v}_{A,B}$  is in the tangent plane at the point of contact  $P$ .

For the rod and washer, the position vector  $\mathbf{r}$  illustrated in Fig. 3 is expressed as

$$\begin{aligned} \mathbf{r} &= (l_1, 0, 0)\mathbf{e} = (l_1 \cos \phi, l_1 \sin \phi, 0)\bar{\mathbf{e}} \\ &= l_1(\cos \theta, -\sin \theta \sin \psi, -\sin \theta \cos \psi)\mathbf{E} \\ &= l_1(\cos \eta \cos \theta + \sin \eta \sin \theta \sin \psi, \sin \eta \cos \theta - \cos \eta \sin \theta \sin \psi, -\sin \theta \cos \psi)\bar{\mathbf{E}}, \end{aligned} \quad (27)$$

where we use Eqs. (15), (16), and (17). The position vector  $\mathbf{r}_t$  displayed in Fig. 3 is expressed as

$$\mathbf{r}_t = (l_3, 0, z)\mathbf{E} = (l_3 \cos \eta, l_3 \sin \eta, z)\bar{\mathbf{E}}, \quad (28)$$

where  $z$  is the height of the point of contact  $P$  with respect to axis  $\mathbf{E}_3$ . The relation  $\mathbf{r}_g = \mathbf{r}_t - \mathbf{r}$  seen in Fig. 3 indicates that  $\mathbf{r}_g$  becomes the following:

$$\mathbf{r}_g = (l_3 - l_1 \cos \theta, l_1 \sin \psi \sin \theta, z + l_1 \cos \psi \sin \theta)\mathbf{E} \quad (29)$$

$$\begin{aligned} &= (l_3 \cos \eta - l_1(\cos \eta \cos \theta + \sin \eta \sin \theta \sin \psi), \\ &\quad l_3 \sin \eta - l_1(\sin \eta \cos \theta - \cos \eta \sin \theta \sin \psi), \\ &\quad z + l_1 \sin \theta \cos \psi)\bar{\mathbf{E}}. \end{aligned} \quad (30)$$

Substitution of Eq. (27) into Eq. (24) yields the following equation:

$$\begin{aligned} \left( \frac{d}{dt} \bar{r}_i(t) \right) \bar{\mathbf{e}}_i(t) &= (-l_1 \dot{\phi} \sin \phi, l_1 \dot{\phi} \cos \phi, 0)_{\bar{\mathbf{e}}} \\ &= (-l_1 \dot{\phi} \cos \psi \sin \eta, l_1 \dot{\phi} \cos \psi \cos \eta, -l_1 \dot{\phi} \sin \psi)_{\bar{\mathbf{E}}}, \end{aligned}$$

where we use Eq. (7), which relates  $\bar{\mathbf{e}}$  to  $\bar{\mathbf{E}}$ . Furthermore, substitution of Eq. (28) into Eq. (25) yields the following equation:

$$\left( \frac{d}{dt} \bar{r}_{ti}(t) \right) \bar{\mathbf{E}}_i = (-l_3 \dot{\eta} \sin \eta, l_3 \dot{\eta} \cos \eta, \dot{z})_{\bar{\mathbf{E}}}.$$

Thus, using Eq. (26), we obtain the constraint condition equations:

$$l_1 \dot{\phi} \cos \psi = \dot{\eta} l_3, \quad (31)$$

$$l_1 \dot{\phi} \sin \psi = -\dot{z}. \quad (32)$$

The equation of the relation between  $\dot{z}$  and  $\dot{\eta}$  is given as

$$\dot{z} = -\dot{\eta} l_3 \tan \psi. \quad (33)$$

If  $\psi$  is a constant, Eq. (33) yields  $z = -\eta l_3 \tan \psi + z_0$ , where  $z_0$  is a constant of integration. This indicates that the locus of the point of contact is a spiral with pitch  $\psi$ . This case is discussed in Section IV.

Differentiation of Eq. (1) and the use of Eqs. (18) and (26) yield

$$\frac{d}{dt} \mathbf{r}_g = \left( \frac{d}{dt} \bar{r}_{ti} \right) \bar{\mathbf{E}}_i - \left( \left( \frac{d}{dt} \bar{r}_i \right) \bar{\mathbf{e}}_i + \boldsymbol{\omega} \times \mathbf{r} \right) = \mathbf{r} \times \boldsymbol{\omega}, \quad (34)$$

from which we find that the velocity of the center of mass is given by the angular velocity.

## B. Angular Velocity

In general, when the relation between  $\bar{\mathbf{e}}$  and  $\bar{\mathbf{E}}$  is given by a matrix  $R$ , as defined by Eq. (7), comparing  $\frac{d}{dt} \bar{\mathbf{e}}_i = \dot{R}_{ij} \bar{\mathbf{E}}_j$  with  $\frac{d}{dt} \bar{\mathbf{e}}_i = \boldsymbol{\omega} \times \bar{\mathbf{e}}_i$  yields the component of the angular velocity  $\boldsymbol{\omega} = (\bar{\omega}_1, \bar{\omega}_2, \bar{\omega}_3)_{\bar{\mathbf{e}}}$  as

$$\epsilon_{ijk} \bar{\omega}_k = (\dot{R}R^t)_{ij},$$

where  $\epsilon$  is the Levi-Civita symbol. The matrix  $\dot{R}R^t$  is found to be an antisymmetric matrix, and the components of the angular velocity  $\boldsymbol{\omega}$  are obtained as

$$\bar{\omega}_1 = (\dot{R}R^t)_{23} = -\dot{\theta} \sin \phi - \dot{\psi} \cos \theta \cos \phi + \dot{\eta} (\sin \phi \sin \psi - \sin \theta \cos \phi \cos \psi),$$

$$\bar{\omega}_2 = (\dot{R}R^t)_{31} = \dot{\theta} \cos \phi - \dot{\psi} \cos \theta \sin \phi - \dot{\eta} (\cos \phi \sin \psi + \sin \theta \sin \phi \cos \psi),$$

$$\bar{\omega}_3 = (\dot{R}R^t)_{12} = -\dot{\phi} - \dot{\psi} \sin \theta + \dot{\eta} \cos \theta \cos \psi,$$

and

$$\omega_1 = -\dot{\psi} \cos \theta - \dot{\eta} \sin \theta \cos \psi, \quad (35)$$

$$\omega_2 = \dot{\theta} - \dot{\eta} \sin \psi, \quad (36)$$

$$\omega_3 = -\dot{\phi} - \dot{\psi} \sin \theta + \dot{\eta} \cos \theta \cos \psi, \quad (37)$$

where we use Eq. (15). We can also obtain the same form of  $\boldsymbol{\omega}$  from the equation as

$$\boldsymbol{\omega} = -\dot{\phi} \mathbf{e}_3 + \dot{\theta} \mathbf{e}_2 - \dot{\psi} \mathbf{E}_1 + \dot{\eta} \mathbf{E}_3.$$

The transformation rules in Eq. (5),

$$\begin{aligned} \mathbf{E}_1 &= \cos \theta \mathbf{e}_1 + \sin \theta \mathbf{e}_3, \\ \mathbf{E}_3 &= -\cos \psi \sin \theta \mathbf{e}_1 - \sin \psi \mathbf{e}_2 + \cos \psi \cos \theta \mathbf{e}_3, \end{aligned} \quad (38)$$

indicate that the components of the angular velocity  $\boldsymbol{\omega} = (\omega_1, \omega_2, \omega_3)_e$  expressed in coordinate frame  $e$  are as follows:

$$\begin{aligned}\omega_1 &= -\dot{\psi} \cos \theta - \dot{\eta} \sin \theta \cos \psi, \\ \omega_2 &= \dot{\theta} - \dot{\eta} \sin \psi, \\ \omega_3 &= -\dot{\phi} - \dot{\psi} \sin \theta + \dot{\eta} \cos \theta \cos \psi.\end{aligned}$$

These equations are equal to Eqs. (35), (36), and (37), respectively.

With the no-slip condition Eq. (31),  $\boldsymbol{\omega}$  becomes

$$\begin{pmatrix} \omega_1 \\ \omega_2 \\ \omega_3 \end{pmatrix} = M \begin{pmatrix} \dot{\phi} \\ \dot{\theta} \\ \dot{\psi} \end{pmatrix}, \quad M \equiv \begin{pmatrix} -\kappa_1 & 0 & -\cos \theta \\ -\kappa_2 & 1 & 0 \\ \kappa_3 & 0 & -\sin \theta \end{pmatrix}, \quad (39)$$

$$\begin{pmatrix} \dot{\phi} \\ \dot{\theta} \\ \dot{\psi} \end{pmatrix} = \frac{1}{\det M} \begin{pmatrix} -\sin \theta & 0 & \cos \theta \\ -\kappa_2 \sin \theta & \det M & \kappa_2 \cos \theta \\ -\kappa_3 & 0 & -\kappa_1 \end{pmatrix} \begin{pmatrix} \omega_1 \\ \omega_2 \\ \omega_3 \end{pmatrix}, \quad (40)$$

$$\det M = \frac{l_1}{l_3} \cos \psi^2 - \cos \theta, \quad (41)$$

where

$$\kappa_1 \equiv \frac{l_1}{l_3} \sin \theta \cos^2 \psi, \quad \kappa_2 \equiv \frac{l_1}{l_3} \cos \psi \sin \psi, \quad \kappa_3 \equiv \frac{l_1}{l_3} \cos \theta \cos^2 \psi - 1. \quad (42)$$

### C. Equations of Motion

The equations of motion of the washer rolling with one point of contact are given as

$$\frac{d}{dt} \mathbf{L} = \mathbf{r} \times \mathbf{f}, \quad (43)$$

$$m \frac{d}{dt} \mathbf{v}_g = \mathbf{f} - m \bar{g} \mathbf{E}_3, \quad (44)$$

where  $\mathbf{L}$  is the angular momentum,  $\mathbf{f}$  is the contact force,  $\mathbf{v}_g \equiv \frac{d}{dt} \mathbf{r}_g$  is the velocity of the center of mass, and  $\bar{g}$  is the gravitational acceleration constant. Substitution of Eq. (44) into Eq. (43) and use of the no-slip condition Eq. (34) yield the equation of motion

$$\frac{d}{dt} \mathbf{L} = \mathbf{r} \times \left( m \frac{d}{dt} (\mathbf{r} \times \boldsymbol{\omega}) + m \bar{g} \mathbf{E}_3 \right). \quad (45)$$

The three components of  $\frac{d}{dt} \mathbf{L}$  are already obtained from Eq. (23). It follows from Eqs. (19) and (20) that

$$\frac{d}{dt} (\mathbf{r} \times \boldsymbol{\omega}) = l_1 (\dot{\phi} \omega_3 + \omega_1^2 + \omega_2^2, -\dot{\omega}_3 - \omega_1 \omega_2, \dot{\omega}_2 - \omega_1 \omega_3)_e.$$

The first term on the right hand side of Eq. (45) can be expressed as

$$\mathbf{r} \times \frac{d}{dt} (\mathbf{r} \times \boldsymbol{\omega}) = l_1^2 (0, \omega_1 \omega_3 - \dot{\omega}_2, -\omega_1 \omega_2 - \dot{\omega}_3)_e.$$

The second term on the right hand side of Eq. (45) can be obtained as

$$m \bar{g} \mathbf{r} \times \mathbf{E}_3 = m \bar{g} (0, -l_1 \cos \theta \cos \psi, -l_1 \sin \psi)_e$$

using  $\bar{\mathbf{E}}_3 = \mathbf{E}_3 = (-\cos \psi \sin \theta, -\sin \psi, \cos \psi \cos \theta)_e$ , which is obtained from Eq. (5). Thus, the three components of Eq. (45) can be expressed as

$$\dot{\omega}_1 = \dot{\phi} \omega_2 + \left( 1 - \frac{I_3}{I_1} \right) \omega_2 \omega_3, \quad (46)$$

$$(I_1 + 1) \dot{\omega}_2 = -I_1 \dot{\phi} \omega_1 + (I_3 + 1 - I_1) \omega_3 \omega_1 - g \cos \theta \cos \psi, \quad (47)$$

$$(I_3 + 1) \dot{\omega}_3 = -\omega_1 \omega_2 - g \sin \psi, \quad (48)$$

where  $I_{1,3} \equiv \bar{I}_{1,3}/ml_1^2$  and  $g \equiv \bar{g}/l_1$ .

### D. Motion Analysis

In this section, we examine the steady precession of the washer, which can be observed in the rotation of an ordinary top.

The initial conditions at  $t = 0$  are given by

$$\dot{\phi}(0) = \dot{\phi}_0 \neq 0, \quad \theta(0) = \theta_0 \neq 0, \quad \psi(0) = 0. \quad (49)$$

We discuss the existence of a steady solution as follows:

$$\theta(t) = \theta_0, \quad \psi(t) = 0, \quad \dot{\phi}(t) = \dot{\phi}_0, \quad \dot{\theta}(t) = \dot{\psi}(t) = 0, \quad \ddot{\theta}(t) = \ddot{\psi}(t) = \ddot{\phi}(t) = 0. \quad (50)$$

Substitution of Eq. (50) into Eq. (39) yields the equations

$$\omega_1 = -\kappa_1 \dot{\phi}, \quad \omega_2 = 0, \quad \omega_3 = \kappa_3 \dot{\phi}. \quad (51)$$

It follows from Eqs. (50) and (42) that  $\dot{\kappa}_i = 0 (i = 1, 2, 3)$  because this term is proportional to  $\dot{\theta}$  and  $\dot{\psi}$ . Thus, the time derivative of Eq. (39) yields

$$\dot{\omega}_1 = -\kappa_1 \ddot{\phi} - \cos \theta \ddot{\psi}, \quad \dot{\omega}_2 = \ddot{\theta}, \quad \dot{\omega}_3 = \kappa_3 \ddot{\phi} - \sin \theta \ddot{\psi}. \quad (52)$$

Substitution of Eqs. (51) and (52) into Eqs. (46), (47), and (48) yields

$$-\kappa_1 \ddot{\phi} - \cos \theta \ddot{\psi} = 0, \quad (53)$$

$$(I_1 + 1)\ddot{\theta} = \kappa_1(I_1 - (I_3 + 1 - I_1)\kappa_3)\dot{\phi}^2 - g \cos \theta \cos \psi_0, \quad (54)$$

$$\kappa_3 \ddot{\phi} - \sin \theta \ddot{\psi} = 0. \quad (55)$$

We observe that the steady solutions  $\ddot{\phi} = \ddot{\psi} = 0$  are consistent with Eqs. (53) and (55). Furthermore, we observe that the steady solution  $\ddot{\theta} = 0$  is consistent with Eq. (54) when  $\dot{\phi}_0^2$  satisfies the condition

$$\dot{\phi}_0^2 = \frac{gl_3 \cos \theta_0}{l_1 \kappa_4 \sin \theta_0}, \quad \kappa_4 \equiv I_1 - \kappa_3(I_3 + 1 - I_1).$$

Next, we discuss steady motion with the condition  $\psi_0 \neq 0$ . In this case, the constraint equation Eq. (33) indicates that the movement in one direction is identical to that in the two points of contact (2PC) mode despite the single point of contact. In the following, we find that this solution does not exist in the 1PC mode. Because  $\kappa_2 = \frac{l_1}{l_3} \cos \psi_0 \sin \psi_0 \neq 0$ , the equation of motion is obtained as

$$-\kappa_1 \ddot{\phi} - \cos \theta \ddot{\psi} = c_1 \dot{\phi}^2, \quad (56)$$

$$(I_1 + 1)(\ddot{\theta} - \kappa_2 \ddot{\phi}) = \kappa_1(I_1 - (I_3 + 1 - I_1)\kappa_3)\dot{\phi}^2 - g \cos \theta \cos \psi_0, \quad (57)$$

$$\kappa_3 \ddot{\phi} - \sin \theta \ddot{\psi} = c_2 \dot{\phi}^2 - c_3, \quad (58)$$

where

$$c_1 \equiv -\frac{\kappa_2}{I_1}(I_1 + \kappa_3(I_1 - I_3)), \quad c_2 \equiv -\frac{1}{I_3 + 1}\kappa_1 \kappa_2, \quad c_3 \equiv \frac{g}{I_3 + 1} \sin \psi_0.$$

Eqs. (56) and (58) can be combined in a matrix form equation for  $\ddot{\psi}$  and  $\ddot{\phi}$ :

$$\begin{pmatrix} -\kappa_1 & -\cos \theta \\ \kappa_3 & -\sin \theta \end{pmatrix} \begin{pmatrix} \ddot{\phi} \\ \ddot{\psi} \end{pmatrix} = \begin{pmatrix} c_1 \dot{\phi}^2 \\ c_2 \dot{\phi}^2 - c_3 \end{pmatrix}. \quad (59)$$

The existence of the steady solution  $\ddot{\psi} = 0, \ddot{\phi} = 0$  in Eq. (59) requires the following relations:

$$\kappa_1 \sin \theta_0 + \kappa_3 \cos \theta_0 = \frac{l_1}{l_3} \cos^2 \psi_0 - \cos \theta_0 \neq 0, \quad (60)$$

$$c_1 \dot{\phi}^2 = 0, \quad (61)$$

$$c_2 \dot{\phi}^2 - c_3 = 0. \quad (62)$$

Eq. (60) is the determinant of the matrix on the left hand side of Eq. (59). From the constraint equation Eq. (71) discussed in Section IV B, we obtain

$$\frac{l_1}{l_3} \cos^2 \psi > \frac{1}{\cos \theta} > 1 > \cos \theta, \quad (63)$$

from which we find that

$$\frac{l_1}{l_3} \cos^2 \psi - \cos \theta > 0$$

and that Eq. (60) is satisfied. The condition  $c_1 = 0$  obtained from Eq. (61) yields

$$I_1 + \kappa_3(I_1 - I_3) = 0 \quad (64)$$

using  $\kappa_2 \neq 0$ . Substitution of  $\ddot{\psi} = 0$ , Eq. (42), Eq. (64), and  $\dot{\phi}^2 = \frac{c_3}{c_2}$ , as obtained from Eq. (62), into Eq. (57) yields

$$\begin{aligned} (I_1 + 1)\ddot{\theta} &= -\kappa_1\kappa_3\dot{\phi}^2 - g \cos \theta_0 \cos \psi_0 \\ &= g \frac{\kappa_3}{\kappa_2} \sin \psi_0 - g \cos \theta_0 \cos \psi_0 \\ &= -g \frac{l_3}{l_1 \cos \psi_0} < 0, \end{aligned}$$

which indicates that the steady solution  $\ddot{\theta} = 0$  with  $\psi_0 \neq 0$  does not exist.

After all, we find that steady precession with a constant value of  $\psi_0 = 0, \theta_0 \neq 0, \dot{\phi}_0^2 = \frac{gl_3 \cos \theta_0}{l_1 \kappa_4 \sin \theta_0}$  exists, but steady precession with a constant value of  $\psi_0 \neq 0$  does not exist.

## IV. MOTION OF THE WASHER WITH TWO POINTS OF CONTACT

### A. Movement of the Washer

We recorded a video with a high-speed camera (CASIO EX-FH20) to observe the movement of the washer. We turned the washer by hand and recorded the video when the velocity of the washer reached terminal velocity. Fig. 11 presents sequential photographs taken at 1/105-s intervals from a video recorded at 420 fps. The washer was composed of 0.7-mm-thick paper, and  $l_1 = 10$  mm and  $l_2 = 2 \times l_1 = 20$  mm. The radius of the wooden rod was  $l_3 = 4$  mm. The sequential photographs of the video indicate that it took 36 frames for the washer to rotate around the rod; therefore, the terminal angular velocity ( $\dot{\eta}_t$ ) was approximately 78 rad/s. Fig. 12 presents sequential photographs of a washer with a smaller radius ( $l_1 = 6$  mm,  $l_2 = 2 \times l_1 = 12$  mm). The time interval was the same as in Fig. 11. The sequential photographs of the video indicate that the terminal angular velocity ( $\dot{\eta}_t$ ) was approximately 156 rad/s. It can be seen that the smaller the radius  $l_1$ , the higher the rotation speed.

Fig. 13 displays the contact of the washer ( $l_1 = 6$  mm) with the rod. It can be seen that there was a small gap between the washer and rod, and that they were in contact at two points. The contact points  $P$  and  $\tilde{P}$  are the points indicated in Fig. 14(d). The exact positions are not known; therefore, the approximate positions are indicated by arrows in Fig. 13.

### B. Constraint Conditions

When there are two points of contact, the constraint conditions of angles  $\theta$  and  $\psi$  are induced from the fact that the washer does not get stuck in the rod.  $Q$  denotes a point on the inner circle of the washer, vector  $\mathbf{r}_q$  denotes  $OQ$ , and vector  $\mathbf{r}_s$  denotes  $GQ$ , as illustrated in Fig. 14(a). The washer is already in contact with the rod at point  $P$ . Vector  $\mathbf{r}_t$  denotes  $OP$ , while vector  $\mathbf{r}$  denotes  $GP$ . When we project the inner diameter of the washer and outer diameter of the rod with radius  $l_3$  onto the plane defined by the unit vectors  $\mathbf{E}_1$  and  $\mathbf{E}_2$ , the curved lines  $C_1$  and  $C_2$  are obtained, respectively, as illustrated in Fig. 14(b). The situation in which the washer gets stuck in the rod is presented in Fig. 14(c). Here, curves  $C_1$  and  $C_2$  intersect at points  $\tilde{P}_1$  and  $\tilde{P}_2$ . The situation in which there are only two points of contact is presented in Fig. 14(d). In this case, points  $\tilde{P}_1$  and  $\tilde{P}_2$  coincide with each other and become point  $\tilde{P}$ .

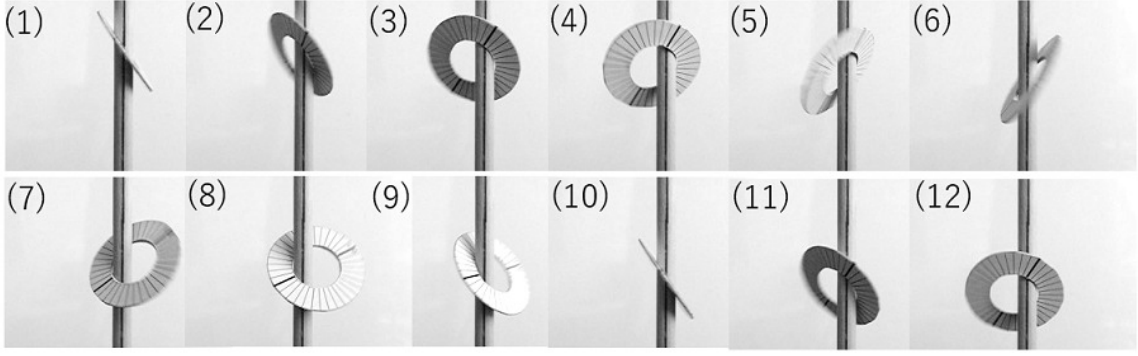


FIG. 11. Sequential photographs of the motion of a washer with radii  $l_1 = 10$  mm and  $l_2 = 20$  mm.

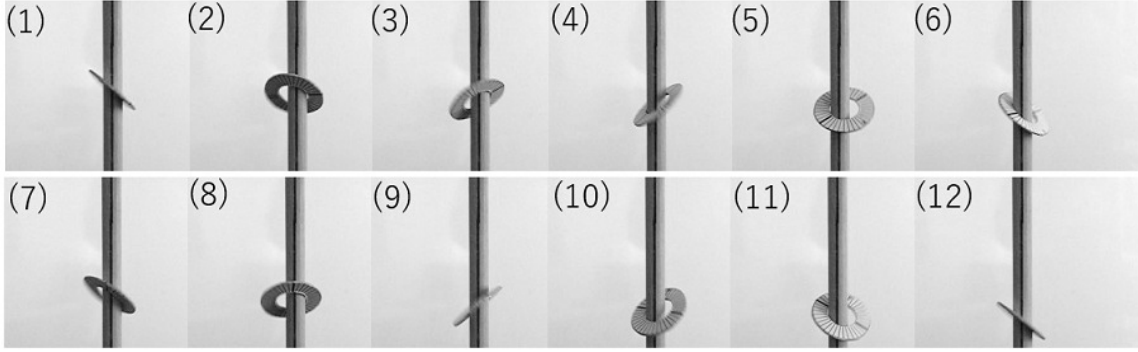


FIG. 12. Sequential photographs of the motion of a washer with radii  $l_1 = 6$  mm and  $l_2 = 12$  mm.

Vector  $\mathbf{r}_s$  is parametrized by  $\alpha$  as follows:

$$\begin{aligned} \mathbf{r}_s(\alpha) &= (l_1 \cos \alpha, l_1 \sin \alpha, 0)_{\mathbf{e}} \quad (\alpha \in [-\pi, \pi]) \\ &= l_1(\cos \alpha \cos \theta, -\cos \alpha \sin \psi \sin \theta + \sin \alpha \cos \psi, -\cos \alpha \cos \psi \sin \theta - \sin \alpha \sin \psi)_{\mathbf{E}}. \end{aligned}$$

Vector  $\mathbf{r}_q$  is given by

$$\mathbf{r}_q = \mathbf{r}_t - \mathbf{r} + \mathbf{r}_s,$$

from which the components with respect to the frame  $\mathbf{E}$  are obtained:

$$\begin{aligned} \mathbf{r}_q &= r_{qi} \mathbf{E}_i, \\ r_{q1} &= l_3 - l_1 \cos \theta + l_1 \cos \alpha \cos \theta, \\ r_{q2} &= l_1 \sin \psi \sin \theta (1 - \cos \alpha) + l_1 \sin \alpha \cos \psi, \\ r_{q3} &= l_1 \cos \psi \sin \theta - l_1 \cos \alpha \cos \psi \sin \theta - l_1 \sin \alpha \sin \psi + z. \end{aligned}$$

Thus, curve  $C_1$  is parametrized by  $\alpha$ :

$$\begin{aligned} C_1(\alpha) &= (r_{q1}(\alpha), r_{q2}(\alpha))_{\mathbf{E}_1 \mathbf{E}_2}, \\ r_{q1}(\alpha) &= l_3 - l_1 \cos \theta + l_1 \cos \alpha \cos \theta, \\ r_{q2}(\alpha) &= l_1 \sin \psi \sin \theta (1 - \cos \alpha) + l_1 \sin \alpha \cos \psi, \end{aligned} \tag{65}$$

from which the curve is found to be an oval by eliminating the parameter  $\alpha$ . When  $\alpha = 0$ , the point on curve  $C_1$  yields

$$C_1(0) = (l_3, 0)_{\mathbf{E}_1 \mathbf{E}_2},$$

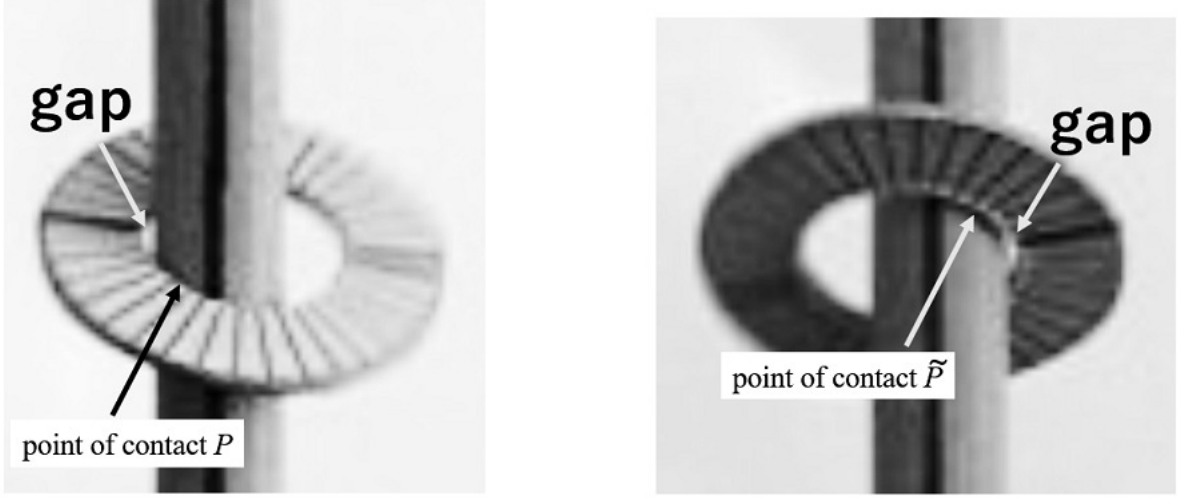


FIG. 13. Small gap between the rod and washer with radius  $l_1 = 6$  mm and points of contact  $P$  and  $\tilde{P}$ .

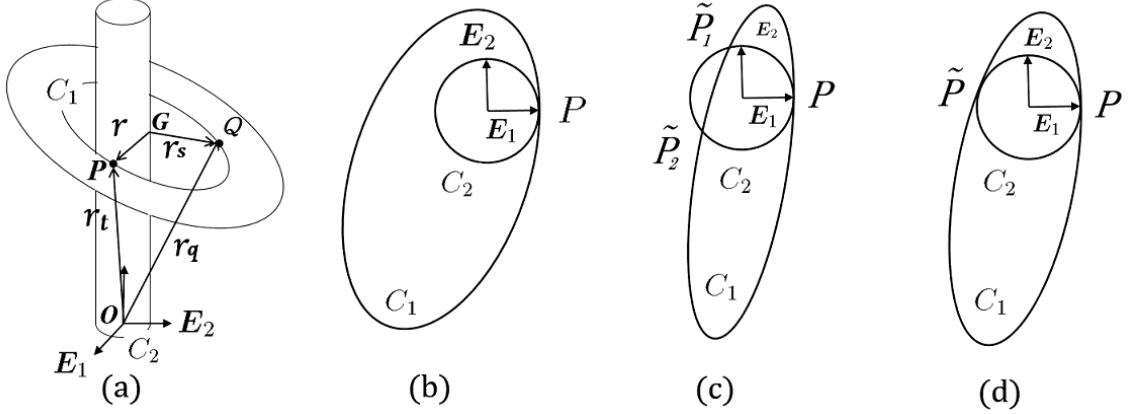


FIG. 14. Washer system with two points of contact (a)  $\mathbf{r}_s = GQ$  and  $\mathbf{r}_q = OQ$ . Curve  $C_1$  is an oval representing the inner diameter of the washer as projected onto the plane defined by the unit vectors  $\mathbf{E}_1$  and  $\mathbf{E}_2$ . Curve  $C_2$  is the outer diameter of the rod. (b) Curve  $C_1$  contacts curve  $C_2$  at one point  $P$  only. (c) The washer gets stuck in the rod. Curves  $C_1$  and  $C_2$  intersect at points  $\tilde{P}_1$  and  $\tilde{P}_2$ . (d) Curves  $C_1$  and  $C_2$  contact each other at point  $\tilde{P}$ . This is the case of two points of contact with the condition  $\tilde{P}_1 = \tilde{P}_2 = \tilde{P}$ .

which describes the point of contact  $P$ . Since points  $\tilde{P}_1$ ,  $\tilde{P}_2$ , and  $\tilde{P}$  are also points on curve  $C_2$ , the solutions corresponding to these points satisfy the equation

$$r_{q1}^2(\alpha) + r_{q2}^2(\alpha) - l_3^2 = 0. \quad (67)$$

Substitution of Eqs. (65) and (66) into Eq. (67) yields the equation

$$(1-u)V(u) = 0, \quad V(u) \equiv d_1 u + d_2 + 2b_1 b_2 \sqrt{1-u^2}, \quad (68)$$

where

$$\begin{aligned} u &\equiv \cos \alpha, \\ d_1 &\equiv -(a^2 + b_1^2 - b_2^2), \quad d_2 \equiv -2l_3 a + a^2 + b_1^2 + b_2^2, \\ a &\equiv l_1 \cos \theta, \quad b_1 \equiv l_1 \sin \psi \sin \theta, \quad b_2 \equiv l_1 \cos \psi. \end{aligned}$$

For  $\psi = 0$ , the situation changes from Fig. 15(a) to Fig. 15(e) as the absolute value of  $\theta$  increases. Figs. 15(d) and 15(e) display the case of becoming stuck in the rod. Fig. 15(c) displays the case of two points of contact, and we find that  $\cos \alpha$  takes the value of  $-1$ . Substitution of  $\cos \alpha = u = -1$  and  $\psi = 0$  into Eq. (68) yields  $\cos \theta_c = \frac{l_3}{l_1}$ .

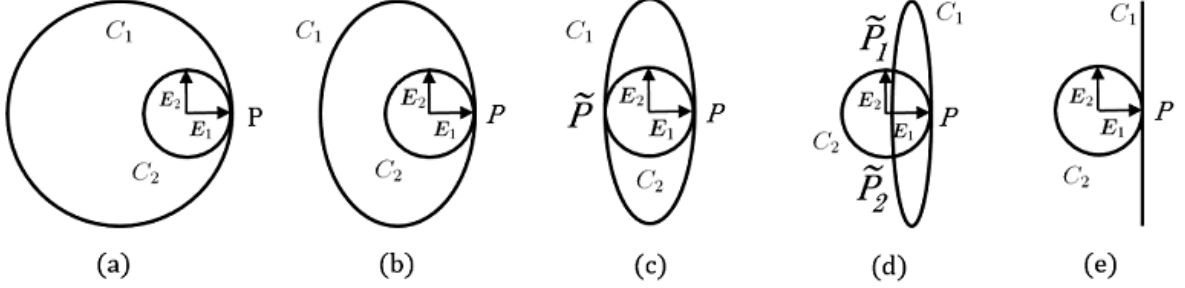


FIG. 15.  $C_1$  and  $C_2$  with  $\psi = 0$  as  $|\theta|$  increases. (a)  $\theta = 0, \cos \theta = 1$ . (b)  $0 < |\theta| < \theta_c, \cos \theta_c = \frac{l_3}{l_1}$ . (c)  $|\theta| = \theta_c$ . (d)  $\theta_c < |\theta| < \frac{\pi}{2}$ . (e)  $|\theta| = \frac{\pi}{2}$ .

For  $\theta = 0$ , the situation changes from Fig. 16(a) to Fig. 16(e) as the absolute value of  $\psi$  increases. Figs. 16(c) and 16(d) display the case of getting stuck in the rod. Fig. 16(b) displays the special case in which  $\tilde{P}_1 = \tilde{P}_2 = \tilde{P} = P$  at  $\alpha = 0$ . Substitution of  $\alpha = 0$  and  $\theta = 0$  into  $V(u) = 0$  yields  $\cos \psi_c = \sqrt{\frac{l_3}{l_1}}$ .

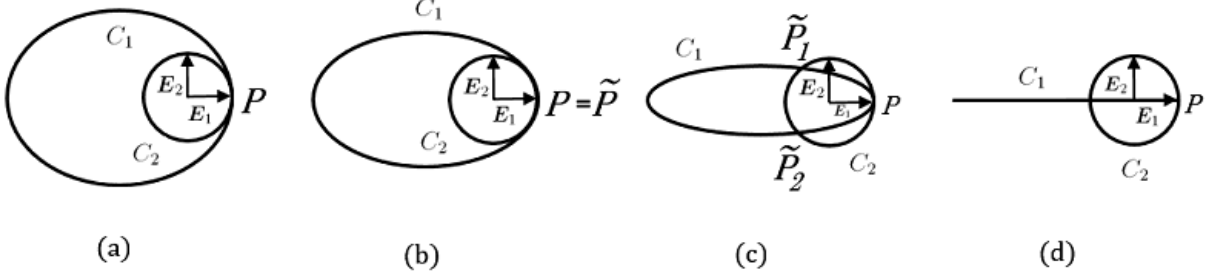


FIG. 16.  $C_1$  and  $C_2$  with  $\theta = 0$  as  $|\psi|$  increases. (a)  $0 < |\psi| < \psi_c, \cos \psi_c = \sqrt{\frac{l_3}{l_1}}$ . (b)  $|\psi| = \psi_c$ . (c)  $\psi_c < |\psi| < \frac{\pi}{2}$ . (d)  $|\psi| = \frac{\pi}{2}$ .

In the case of  $0 < \psi \leq \psi_c$  and  $0 < \theta \leq \theta_c$ , when equation  $V(u) = 0$  has multiple roots, the roots correspond to the point of contact  $\tilde{P}$ . Squaring  $V(u) = 0$  gives

$$(d_1^2 + 4b_1^2 b_2^2)u^2 + 2d_1 d_2 u + \alpha^2 - 4b_1^2 b_2^2 = 0.$$

The condition in which the discriminant is equal to zero gives

$$d_1^2 - d_2^2 + 4b_1^2 b_2^2 = 0. \quad (69)$$

The constraint condition obtained from Eq. (69) is

$$\frac{l_3}{l_1} - \cos^2 \psi \cos \theta = 0 \quad (70)$$

by dividing by the factor  $4l_1^4 \cos \theta \left(1 - \frac{l_3}{l_1} \cos \theta\right) > 0$  because  $\frac{l_3}{l_1} < 1$ . The physical condition that the washer does not get stuck in the rod leads to the inequality

$$\frac{l_3}{l_1} - \cos^2 \psi \cos \theta \leq 0. \quad (71)$$

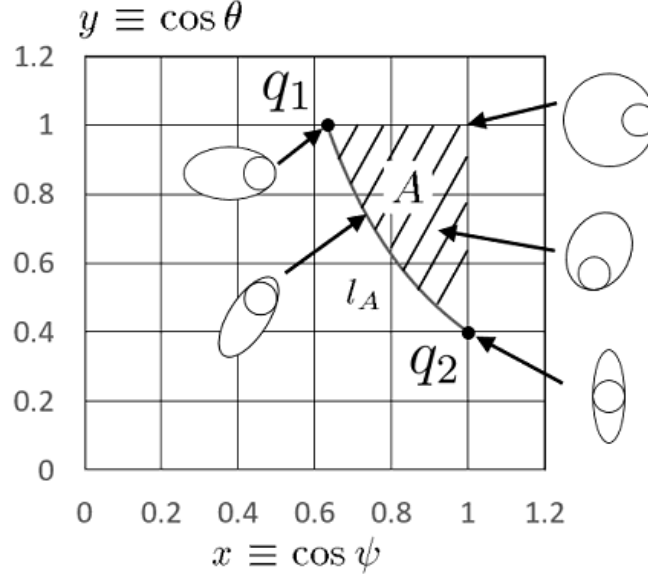


FIG. 17. The black curve is drawn at values of  $l_1 = 10$  mm and  $l_3 = 4$  mm. Area  $A$  corresponds to the inequality  $\frac{l_3}{l_1} - \cos^2 \psi \cos \theta \leq 0$ , and  $l_A$  is the boundary line of area  $A$ , on which there are only two points of contact. Point  $q_1$  is on the line with  $\theta = 0$ , at which the value of  $\psi_c$  is given by  $\cos \psi_c = \sqrt{\frac{l_3}{l_1}}$ . Point  $q_2$  is on the line with  $\psi = 0$ , at which the value of  $\theta_c$  is given by  $\cos \theta_c = \frac{l_3}{l_1}$ .

An area satisfying Eq. (71) corresponds to  $A$  in Fig. 17, where  $x \equiv \cos \psi$  and  $y \equiv \cos \theta$ . The values of  $l_1$  and  $l_3$  are set to  $l_1 = 10$  mm and  $l_3 = 4$  mm, respectively. The border line is  $l_A$ , corresponding to Eq. (70). Points  $q_1$  and  $q_2$  are on the line  $l_A$  with  $y = 1$  and  $x = 1$ , respectively. Point  $q_1$  has the component  $q_1 = (\cos \psi_c = \sqrt{\frac{l_3}{l_1}}, 1)$ , corresponding to Fig. 16(b), while point  $q_2$  has the component  $q_2 = (1, \cos \theta_c = \frac{l_3}{l_1})$  corresponding to Fig. 15(c).

### C. Equations of Motion

We obtain the equations of motion of the washer at two points of contact  $P$  and  $\tilde{P}$  without slipping, as illustrated in Fig. 18. The position vectors of the points of contact  $P$  and  $\tilde{P}$  are  $\mathbf{r}_1$  and  $\mathbf{r}_2$ , respectively.

Because the washer rotates around the axis that passes through the points of contact  $P$  and  $\tilde{P}$ , the unit vector with respect to the direction of this axis is  $\tilde{\mathbf{e}}_1$ , as indicated in Fig. 18(a). Axis  $\tilde{\mathbf{e}}_3$  is the same as  $\mathbf{e}_3$ , and axis  $\tilde{\mathbf{e}}_2$  is obtained by  $\tilde{\mathbf{e}}_2 = \tilde{\mathbf{e}}_3 \times \tilde{\mathbf{e}}_1$ .

Vector  $\mathbf{E}_{3p}$  is defined by vector  $\mathbf{E}_3$ , namely, Eq. (38) projected onto the plane defined by the unit vectors  $\mathbf{e}_1$  and  $\mathbf{e}_2$ , as illustrated in Fig. 18(b), and is given by

$$\mathbf{E}_{3p} = (-\rho_1, -\rho_2, 0)\mathbf{e},$$

where  $\rho_1$  and  $\rho_2$  are defined as

$$\rho_1 \equiv \sin \theta \cos \psi, \quad \rho_2 \equiv \sin \psi.$$

We find that  $\tilde{\mathbf{e}}_1$  is a unit vector with the opposite direction to that of  $\mathbf{E}_{3p}$ . Thus,  $\tilde{\mathbf{e}}_1$  is obtained as

$$\tilde{\mathbf{e}}_1 = \frac{1}{\rho}(\rho_1, \rho_2, 0)\mathbf{e},$$

where

$$\rho \equiv \sqrt{\rho_1^2 + \rho_2^2} = \sqrt{1 - \rho_3^2}, \quad \rho_3 \equiv \cos \theta \cos \psi.$$

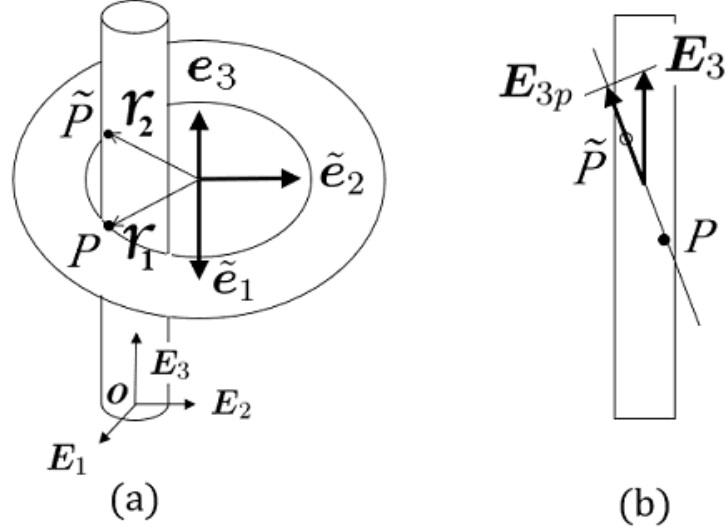


FIG. 18. Washer with two points of contact with the rod. (a) The two points of contacts are  $P$  and  $\tilde{P}$ , while  $\mathbf{r}_1$  and  $\mathbf{r}_2$  are the position vectors at  $P$  and  $\tilde{P}$ , respectively. The direction of  $\tilde{\mathbf{e}}_1$  is parallel to the direction from  $\tilde{P}$  to  $P$ . The axis  $\tilde{\mathbf{e}}_3$  is the same as  $\mathbf{e}_3$ . (b) Vector  $\mathbf{E}_{3p}$  is defined by the vector  $\mathbf{E}_3$

It follows from  $\tilde{\mathbf{e}}_2 = \mathbf{e}_3 \times \tilde{\mathbf{e}}_1$  that  $\tilde{\mathbf{e}}_2$  is calculated as

$$\tilde{\mathbf{e}}_2 = \frac{1}{\rho}(-\rho_2, \rho_1, 0)\mathbf{e}.$$

The relations between  $\tilde{\mathbf{e}}_i$ ,  $\mathbf{e}_i$ , and  $\mathbf{E}$  are obtained as follows:

$$\mathbf{e}_i = \tilde{R}_{ij}\tilde{\mathbf{e}}_j, \quad \tilde{\mathbf{e}}_i = \tilde{R}_{ij}^{-1}\mathbf{e}_j, \quad (72)$$

$$\tilde{R} = \frac{1}{\rho} \begin{pmatrix} \rho_1 & -\rho_2 & 0 \\ \rho_2 & \rho_1 & 0 \\ 0 & 0 & \rho \end{pmatrix}, \quad \tilde{R}^{-1} = \frac{1}{\rho} \begin{pmatrix} \rho_1 & \rho_2 & 0 \\ -\rho_2 & \rho_1 & 0 \\ 0 & 0 & \rho \end{pmatrix},$$

$$\begin{aligned} \mathbf{E}_i &= R_{1\psi ij} R_{2\theta jk} \tilde{R}_{kl} \tilde{\mathbf{e}}_l \\ &= \frac{1}{\rho} \begin{pmatrix} \cos \theta \rho_1 & -\cos \theta \rho_2 & \sin \theta \rho \\ \cos^2 \theta \cos \psi \sin \psi & \sin \theta & \sin \psi \cos \theta \rho \\ -\rho^2 & 0 & \rho_3 \rho \end{pmatrix}_{ij} \tilde{\mathbf{e}}_j. \end{aligned} \quad (73)$$

The components of vectors  $\mathbf{r}_1$  and  $\mathbf{r}_2$  with respect to frame  $\tilde{\mathbf{e}}_i$  are obtained using Eq. (72):

$$\mathbf{r}_1 = (l_1, 0, 0)\mathbf{e} = \frac{l_1}{\rho}(\rho_1, -\rho_2, 0)\tilde{\mathbf{e}}, \quad \mathbf{r}_2 = -\frac{l_1}{\rho}(\rho_1, \rho_2, 0)\tilde{\mathbf{e}}. \quad (74)$$

The forces  $\mathbf{f}_1$  and  $\mathbf{f}_2$  acting at the points of contact  $P_1$  and  $P_2$ , respectively, have components denoted by

$$\mathbf{f}_i = ml_1(\tilde{f}_{i1}, \tilde{f}_{i2}, \tilde{f}_{i3})\tilde{\mathbf{e}}.$$

The components of the torque  $\mathbf{N} = \tilde{N}_i\tilde{\mathbf{e}}_i$  are obtained as

$$\begin{aligned} \mathbf{N} &= \mathbf{r}_1 \times \mathbf{f}_1 + \mathbf{r}_2 \times \mathbf{f}_2, \\ \tilde{N}_1 &= -\frac{ml_1^2}{\rho}\rho_2(\tilde{f}_{13} + \tilde{f}_{23}), \\ \tilde{N}_2 &= -\frac{ml_1^2}{\rho}\rho_1(\tilde{f}_{13} - \tilde{f}_{23}), \\ \tilde{N}_3 &= -\frac{ml_1^2}{\rho}(\rho_1(-\tilde{f}_{12} + \tilde{f}_{22}) - \rho_2(\tilde{f}_{11} + \tilde{f}_{21})). \end{aligned}$$

We obtain the angular velocity components as follows:  $\boldsymbol{\omega} = (\tilde{\omega}_1, \tilde{\omega}_2, \tilde{\omega}_3)_{\tilde{\mathbf{e}}}$ . Under the no-slip condition, velocity  $\mathbf{v}_g$  is expressed as

$$\mathbf{v}_g = \mathbf{r}_1 \times \boldsymbol{\omega} = \mathbf{r}_2 \times \boldsymbol{\omega},$$

from which we obtain the relation

$$(\mathbf{r}_1 - \mathbf{r}_2) \times \boldsymbol{\omega} = 0. \quad (75)$$

Furthermore, since

$$\mathbf{r}_1 - \mathbf{r}_2 = \frac{l_1}{\rho}(2\rho_1, 0, 0)_{\tilde{\mathbf{e}}} \quad (76)$$

from Eq. (74), we obtain

$$(\mathbf{r}_1 - \mathbf{r}_2) \times \boldsymbol{\omega} = \frac{l_1}{\rho}(0, -2\rho_1\tilde{\omega}_3, 2\rho_1\tilde{\omega}_2)_{\tilde{\mathbf{e}}}. \quad (77)$$

From Eqs. (75) and (77), we find that

$$\tilde{\omega}_2 = \tilde{\omega}_3 = 0. \quad (78)$$

The equation  $(\mathbf{r}_1 - \mathbf{r}_2) \times \boldsymbol{\omega} = 0$  signifies that the direction of  $(\mathbf{r}_1 - \mathbf{r}_2)$  is parallel to the direction of  $\boldsymbol{\omega}$ ; thus,  $(\mathbf{r}_1 - \mathbf{r}_2)$  is the rotation axis. Axis  $\tilde{\mathbf{e}}_1$  is parallel to the direction of  $(\mathbf{r}_1 - \mathbf{r}_2)$ ; thus,  $\tilde{\omega}_1$  has a nonzero value, and the other directions have zero components:  $\tilde{\omega}_2 = \tilde{\omega}_3 = 0$ .

Furthermore, we can demonstrate that angles  $\psi$  and  $\theta$  have constant values in the 2PC mode under the no-slip condition.  $\tilde{\omega}_2$  and  $\tilde{\omega}_3$  are the functions of variables  $\dot{\phi}$ ,  $\dot{\psi}$ ,  $\dot{\theta}$ , and  $\dot{\eta}$  as follows:

$$\begin{aligned} \tilde{\omega}_2 &= \frac{1}{\rho}(-\rho_2\omega_1 + \rho_1\omega_2) \\ &= \dot{\eta}(\rho_2 \sin \theta \cos \psi - \rho_1 \sin \psi) + \rho_1 \dot{\theta} \\ &= \rho_1 \dot{\theta}, \end{aligned} \quad (79)$$

$$\begin{aligned} \tilde{\omega}_3 &= \omega_3 = \frac{\dot{\eta}}{\cos \theta} \left(-\frac{l_3}{l_1} + \cos^2 \psi \cos \theta\right) + \dot{\psi} \sin \theta \\ &= \dot{\psi} \sin \theta, \end{aligned} \quad (80)$$

where we use the expression of  $\omega_i$  in Eq. (39), the relation equation between  $\mathbf{e}$  and  $\tilde{\mathbf{e}}$  in Eq. (72), and the constraint condition in Eq. (70). From Eq. (79), Eq. (80), and  $\tilde{\omega}_2 = \tilde{\omega}_3 = 0$  obtained in Eq. (78), we find that  $\dot{\psi} = \dot{\theta} = 0$ ; thus,  $\psi$  and  $\theta$  have constant values in the 2PC mode.

It follows from  $\dot{\psi} = \dot{\theta} = 0$  that  $\omega_1 = -\dot{\eta} \sin \theta \cos \psi$  and  $\omega_2 = -\dot{\eta} \sin \psi$ , from which we obtain

$$\begin{aligned} \tilde{\omega}_1 &= \frac{1}{\rho}(\rho_1\omega_1 + \rho_2\omega_2) \\ &= -\frac{\dot{\eta}}{\rho}(\rho_1 \sin \theta \cos \psi + \rho_2 \sin \psi) = -\dot{\eta}\rho. \end{aligned} \quad (81)$$

Under the no-slip condition, the angular velocity is as follows:

$$\boldsymbol{\omega} = (-\dot{\eta}\rho, 0, 0)_{\tilde{\mathbf{e}}}. \quad (82)$$

The angular momentum  $\mathbf{L} = \tilde{L}_i \tilde{\mathbf{e}}_i$  is obtained using Eqs. (22) and (72):

$$\tilde{L}_1 = \bar{I}_1 \tilde{\omega}_1, \quad \tilde{L}_2 = \tilde{L}_3 = 0.$$

It follows from Eqs. (23) and (72) that the time derivative of the angular momentum is

$$\frac{d}{dt} \mathbf{L} = (\bar{I}_1 \dot{\tilde{\omega}}_1, \bar{I}_1 \dot{\phi} \tilde{\omega}_1, 0)_{\tilde{\mathbf{e}}} = -\bar{I}_1(\rho \dot{\eta}, \rho \rho_3 \dot{\eta}^2, 0)_{\tilde{\mathbf{e}}},$$

where we use Eq. (31), Eq. (81), and  $\dot{\rho} = 0$  because  $\dot{\psi} = \dot{\theta} = 0$ . Thus, the equations of motion with respect to the angular momentum  $\frac{d}{dt}\mathbf{L} = \mathbf{N}$  can be expressed as

$$I_1\rho\ddot{\eta} = \frac{1}{\rho}\rho_2(\tilde{f}_{13} + \tilde{f}_{23}), \quad (83)$$

$$I_1\rho\rho_3\dot{\eta}^2 = \frac{1}{\rho}\rho_1(\tilde{f}_{13} - \tilde{f}_{23}), \quad (84)$$

$$0 = \rho_1(-\tilde{f}_{12} + \tilde{f}_{22}) - \rho_2(\tilde{f}_{11} + \tilde{f}_{21}). \quad (85)$$

The equation of motion of the center of mass is given by

$$m\frac{d^2}{dt^2}\mathbf{r}_g = \mathbf{f}_1 + \mathbf{f}_2 - m\bar{g}\mathbf{E}_3.$$

The acceleration  $\frac{d^2}{dt^2}\mathbf{r}_g$  is calculated from Eq. (34) as follows:

$$\frac{d^2}{dt^2}\mathbf{r}_g = -l_1\rho_2(\ddot{\eta}\tilde{\mathbf{e}}_3 + \rho\dot{\eta}^2\tilde{\mathbf{e}}_2).$$

The components of  $\mathbf{E}_3$  in frame  $\tilde{\mathbf{e}}$  are obtained from Eq. (73) as  $\mathbf{E}_3 = (-\rho, 0, \rho_3)\tilde{\mathbf{e}}$ . Consequently, the equations of motion with respect to the center of mass are given by

$$0 = \tilde{f}_{11} + \tilde{f}_{21} + g\rho, \quad (86)$$

$$\rho\rho_2\dot{\eta}^2 = -\tilde{f}_{12} - \tilde{f}_{22}, \quad (87)$$

$$\rho_2\ddot{\eta} = -\tilde{f}_{13} - \tilde{f}_{23} + g\rho_3. \quad (88)$$

Eqs. (83) and (84) can be combined in the equations for  $\tilde{f}_{13}$  and  $\tilde{f}_{23}$ :

$$\tilde{f}_{13} = \frac{I_1\rho^2}{2}\left(\frac{C_0}{\rho_2} + \frac{\rho_3\dot{\eta}^2}{\rho_1}\right), \quad \tilde{f}_{23} = \frac{I_1\rho^2}{2}\left(\frac{C_0}{\rho_2} - \frac{\rho_3\dot{\eta}^2}{\rho_1}\right). \quad (89)$$

Substitution of Eq. (86) into Eq. (85) and the use of Eq. (87) yield

$$\tilde{f}_{12} = -\frac{\rho\rho_2}{2}\left(\dot{\eta}^2 - \frac{g}{\rho_1}\right), \quad \tilde{f}_{22} = -\frac{\rho\rho_2}{2}\left(\dot{\eta}^2 + \frac{g}{\rho_1}\right). \quad (90)$$

For each force,  $\tilde{f}_{11}$  and  $\tilde{f}_{21}$  are not given by the equations of motion. Since only the sum is obtained by Eq. (86) as  $\tilde{f}_{11} + \tilde{f}_{21} = -g\rho$ , we introduce a parameter  $\delta$  and set the force  $\tilde{f}_{11}$  and  $\tilde{f}_{21}$  as follows:

$$\tilde{f}_{11} = -g\delta\rho, \quad \tilde{f}_{21} = -g(1 - \delta)\rho. \quad (91)$$

The forces exerted by the rod are illustrated in Fig. 19.

#### D. Motion Analysis

We discuss the motion of the washer based on the forces obtained above. In the following discussion, we assume that the angles have a constant positive value:

$$\theta_0 > 0, \quad \psi_0 > 0, \quad (92)$$

as illustrated in Fig. 8(4) and Fig. 18.

Since angles  $\phi$  and  $\theta$  are constant values, the components of the center of mass with respect to frame  $\mathbf{E}$ , given by Eq. (29), are also constant values, from which the motion of the center of mass projected onto the plane of  $\tilde{\mathbf{E}}_1$  and  $\tilde{\mathbf{E}}_2$  is found to be a circular motion with angular velocity  $\dot{\eta}$ . The centripetal force is  $\tilde{f}_{12} + \tilde{f}_{22}$ , given by

$$\tilde{f}_{12} + \tilde{f}_{22} = -\rho\rho_2\dot{\eta}^2.$$

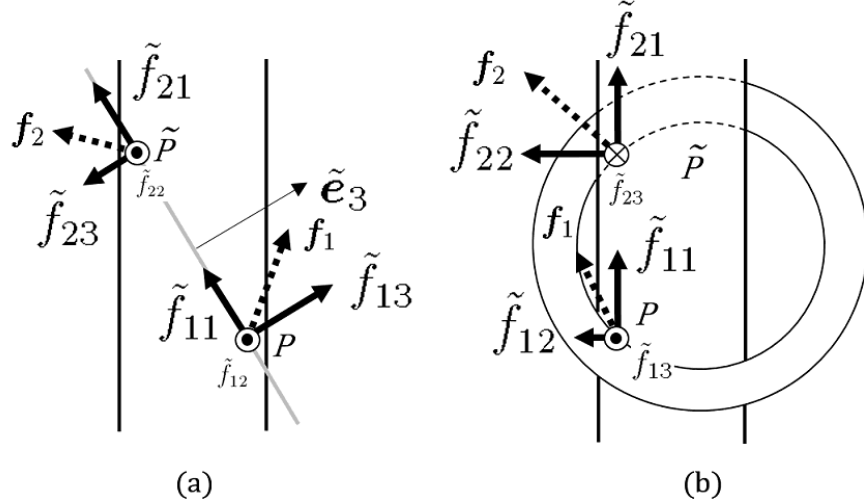


FIG. 19. Forces exerted by the rod. (a) Dotted lines represent  $f_1$  and  $f_2$ .  $\tilde{f}_{13}$  and  $\tilde{f}_{23}$  are represented by Eq. (89) when  $\tilde{f}_{23}$  has a negative value. We assume that  $\delta = 0.5$ ; then,  $\tilde{f}_{11} = \tilde{f}_{21} < 0$  because only the sum of these forces is given. (b)  $\tilde{f}_{12}$  and  $\tilde{f}_{22}$  are represented by Eq. (90).

Substitution of Eq. (88) into Eq. (83) yields the equation

$$\ddot{\eta} = C_0, \quad C_0 \equiv \frac{g\rho_2\rho_3}{\rho_2^2 + I_1\rho^2}. \quad (93)$$

It follows from Eq. (92) that  $\rho_2 > 0$  and  $\rho_3 > 0$ ; thus,  $C_0$  has a positive constant value. The acceleration with respect to  $\eta$  is constant, from which the motion of the washer is identical to free fall motion. Thus, at time  $t = 0$ , when the washer begins to make contact at two points,  $\eta(t)$  can be obtained as

$$\eta(t) = \eta(0) + \dot{\eta}(0)t + \frac{1}{2}C_0t^2, \quad (94)$$

where  $\eta(0)$  and  $\dot{\eta}(0)$  are the initial values. The constraint condition in Eq. (33) indicates that the locus of the point of contact is a spiral with a pitch given by the angle  $\psi$ . The angular velocity increases because the potential energy is converted into kinetic energy as in free fall. In practice, the angular velocity reaches a constant value (terminal velocity  $\dot{\eta}_t$ ) due to energy dissipation caused by factors such as rolling friction, air viscosity, and sound as follows:

$$\eta(t) = \eta(0) + \dot{\eta}_t t. \quad (95)$$

Even if the gravity constant is equal to zero,  $g = 0$  ( $C_0 = 0$ ), angle  $\eta(t)$  increases linearly with time  $t$  from Eq. (94). This motion can be observed when the rod is placed horizontally and the washer is initially rotated by hand. To be precise, even if the rod are parallel, gravity acts on the washer, but there is no gravity component in the direction of motion.

We simulated the motion of a washer with  $l_1 = 10$  mm,  $l_2 = 20$  mm, and  $l_3 = 4$  mm using Eqs. (7), (30), (33), and (95). In this simulation, we required constant values of  $\dot{\eta}_t$ ,  $\psi$ , and  $\theta$ , and these values were obtained as follows. The value of  $\dot{\eta}_t \sim 78$  rad/s was obtained as described in Section IV A. By observing how the thin lines drawn on the washer every 10 degrees moved, the increase in the angle  $\phi$  was determined. It can be seen from video by which Fig. 11 is obtained that  $\phi$  increased by almost  $\pi$  rad in the time (36 frames) that  $\eta$  increased by almost  $2\pi$  rad. Under the no-slip condition Eq. (32), the value of  $\psi$  was obtained: approximately 0.64 rad. Using the 2PC constraint condition Eq. (70), the value of  $\theta$  was obtained: approximately 0.9 rad. For the numerical simulation, the NDSolve command in Mathematica (Wolfram Research Inc.) was used. The Mathematica file is available on the author's website [16]. Fig. 20(a) is identical to Fig. 11(a). Fig. 20(b) presents the numerical simulation, and it can be seen that the behavior is very similar to that displayed in Fig. 20(a).

The washer falls with  $\theta > 0$ ,  $\psi > 0$ , which can be understood by moving the rod and washer by hand. As displayed in Fig. 21, when rotating the rod in the direction of arrow  $A$  using the left hand (washer rotates in the opposite direction) and at the same time rotating the washer in the direction of arrow  $B$  using the right hand, it can be seen

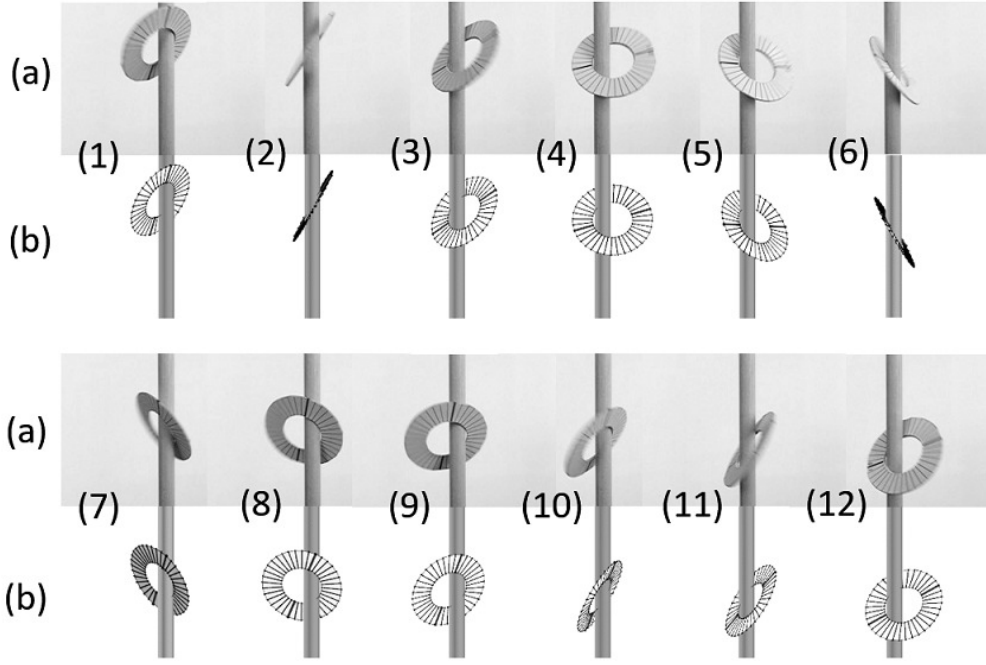


FIG. 20. Comparison of photographs and simulation results of washer motion. (a) The same sequential photographs as in Fig. 11. (b) Sequential images of the washer motion obtained by numerical simulation.

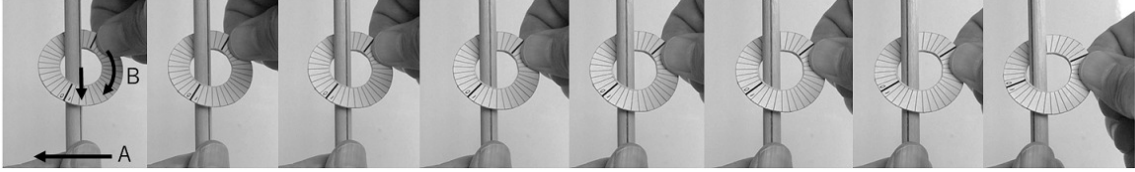


FIG. 21. Rotation of the rod in direction  $A$  using the left hand and of the washer in direction  $B$  using the right hand. The washer moves downward as a result.

that the washer moves downward. The combination of the rotation  $B$  and opposite rotation of  $A$  yields  $\tilde{\omega}_1 \neq 0$  and  $\tilde{\omega}_{2,3} = 0$ , as expressed in Eq. (82).

If the sign of angle  $\psi > 0$  changes to  $\psi < 0$  for some reason, the position velocity  $\dot{z}$  becomes positive with  $\dot{z} = -l_3 \dot{\eta} \tan \psi > 0$ . Then, the phenomenon of the falling washer suddenly moving upward can be observed. This phenomenon can be seen in the "rock the baby" movement, which is a trick performed with chatter ring. This phenomenon has been reported in the case of two washers colliding [17].

## V. CONCLUSIONS AND DISCUSSION

To understand the motion of the small rings of the chatter ring, our model, which consists of a straight rod and a washer ring, is analyzed under the no-slip condition. The equations of motion and constraint conditions in both the 1PC and 2PC modes are obtained. In the 1PC mode, the motion of the washer is similar to that of a hula hoop, and the steady precession of the washer occurs under the condition  $\theta(0) \neq 0, \psi(0) = 0$  but not under the condition  $\theta(0) \neq 0, \psi(0) \neq 0$ . In the 2PC mode, the locus of the point of contact is a spiral with a pitch given by the angle  $\psi$ , and the acceleration with respect to  $\eta$  is found to be constant, from which the motion of the washer is identical to free fall motion. The motion of the small ring of the chatter ring is similar to that of the washer in the 2PC mode as observed with a high-speed camera. Thus, the motion of a hula hoop is different from that of the chatter ring. The motion of the washer consists of rotation around the axis that passes through the points of contact  $P$  and  $\bar{P}$ . The motion of the center of mass projected onto the horizontal plane defined by unit vectors  $\bar{\mathbf{E}}_1$  and  $\bar{\mathbf{E}}_2$  is a circle, and the

angular velocity increases because the potential energy is converted into kinetic energy in the same way as free fall. In practice, the angular velocity reaches a constant value via energy dissipation due to rolling friction, air viscosity, sound, and other factors. The components of the forces received from the rod at the points of contact, which are normal to the plane of the washer, induce part of the acceleration  $\ddot{y}$ . The sum of the components of the forces parallel to the horizontal plane are centripetal forces, which induce circular motion of the center of mass projected onto the plane defined by unit vectors  $\bar{E}_1$  and  $\bar{E}_2$ .

In Section IV A, the motion of a washer with  $l_1 = 6$  mm and  $l_1 = 10$  mm is described. However, under the condition of  $l_2 = 2l_1$ , other washers with  $l_1 = 5$  mm, 8 mm, 12 mm, 14 mm, 15 mm, 16 mm and 18 mm were also created and turned. At  $l_1 = 5$  mm, downward motion was observed with almost no rotation, while at  $l_1 = 16$  mm and 18 mm, downward motion with slipping and rotation was observed. Videos are available on the author's website [16].

In addition, there are two non-dimensional parameters related to the size of the washer and rod:  $l_2/l_1$  and  $l_3/l_1$ . There seems to be a range of the parameters that turns well and does not slip. This has also been reported in a previous paper [13]. Future work will clarify the reasons why the washer turns or does not turn well.

## ACKNOWLEDGMENTS

The author would like to thank M. Sakamoto (Department of Physics, Kobe University, Japan) for showing him the curious movement of the small ring of the chatter ring. The author would also like to thank the members of the elementary particle physics groups at Niigata University and Yamagata University for their valuable comments during the autumn seminar at Iide Yamagata in Japan (2015). The author also appreciates the support received at a workshop hosted by the Yukawa Institute for Theoretical Physics at Kyoto University.

- 
- [1] Walker, G. T., On a Dynamical Top, *Quarterly Journal of Pure and Applied Mathematics*, 1896, vol. 28, pp. 175–184.
  - [2] Moffatt, H. K. and Tokieda, T., Celt Reversals: A Prototype of Chiral Dynamics, *Proc. R. Soc. Edinburgh. A*, 2008, vol. 138, pp. 361–368.
  - [3] Borisov, A. V. and Mamaev, I. S., Strange Attractors in Rattleback Dynamics, *Physics-Uspeski*, 2003, vol. 46 (4), pp. 393–403.
  - [4] Takano, H., Spin Reversal of a Rattleback with Viscous Friction, *Regular and Chaotic Dynamics*, 2014, vol. 19 (1), pp. 81–99.
  - [5] Japan Chatter Ring Association Home Page, <<http://jaringa.web.fc2.com/index-e.html>>.
  - [6] Sato, K., He is a music composer and a kinetic artist in Japan (1927–2009). His works are located in the Museum of Fine Arts, Gifu and can be seen on YouTube, <<https://www.youtube.com/watch?v=g2005Vp6qDg>>.
  - [7] Rod, C., Effect of friction on a hula hoop, *Physics Education*, 2021, vol. 56, pp. 1–4.
  - [8] Borisov, A. V. and Mamaev, I. S., The Rolling Motion of a Rigid Body on a Plane and a Sphere: Hierarchy of Dynamics, *Regular and Chaotic Dynamics*, 2002, vol. 7 (2), pp. 177–200.
  - [9] Routh, E. J., *The Advanced Part of a Treatise on the Dynamics of a System of Rigid Bodies*, Macmillan, 1884.
  - [10] Neimark, J. I. and Fufaev, N. A., *Dynamics of Nonholonomic Systems*, American Mathematical Society, 1972.
  - [11] Borisov, A. V., Mamaev, I. S. and Kilin, A. A., The Rolling Motion of a Ball on a Surface: New Integrals and Hierarchy of Dynamics, *Regular and Chaotic Dynamics*, 2002, vol. 7 (2), pp. 201–219.
  - [12] Gualtieri, M., Tokieda, T., Advis-Gaete, L., Carry, B., Reffet, E. and Guthmann, C., Golfer's Dilemma, *Am. J. Phys.*, 2006, vol. 74 (6), pp. 497–501.
  - [13] Crane, H. R., Chattering, the Chattering, and the Hula Hoop, *The Physics Teacher*, 1992, vol. 30, pp. 306–308.
  - [14] Hunt, H., Home Page, DYNAMICS MOVIES/Wobblers <<http://www3.eng.cam.ac.uk/~hemh1/movies.htm>>.
  - [15] Fahnlne, D. E., Home Page, <<https://www.rose-hulman.edu/~moloney/AppComp/2001Entries/e04a/chatteringtoy.htm>>.
  - [16] Takano, H., Home Page, <<http://www.juen.ac.jp/lab/takano>>.
  - [17] Walker, J., *The Flying Circus of Physics with Answers*, John Wiley & Sons, 1977.